

AD-A138 290

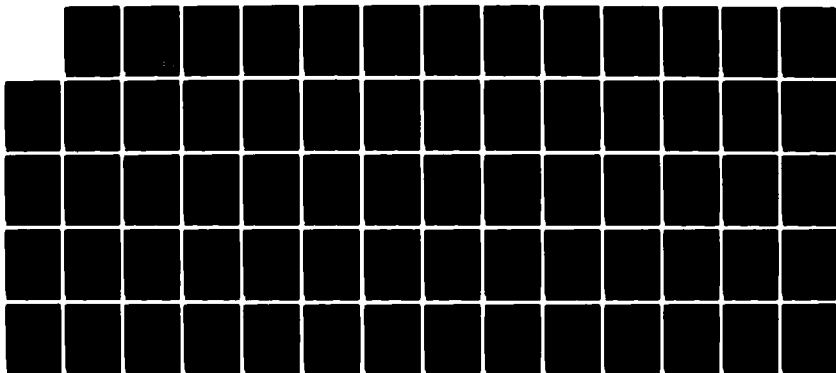
REFRACTION DUE TO SHOCK WAVES(U) MISSION RESEARCH CORP
SANTA BARBARA CA T J BARRETT ET AL. 01 MAR 83
MRC-R-743 DNA-TR-82-132 DNA001-82-C-0197

1/1

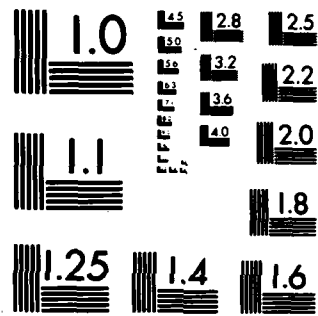
UNCLASSIFIED

F/G 18/3

NL



END
DATE
FILMED
3 84
DTIC



MICROCOPY RESOLUTION TEST CHART
NATIONAL BUREAU OF STANDARDS-1963-A

AD-E301328

12

ADA138290

DNA-TR-82-132

REFRACTION DUE TO SHOCK WAVES

Thomas J. Barrett
Russell H. Christian
Mission Research Corporation
P.O. Drawer 719
Santa Barbara, California 93102

1 March 1983

Technical Report

CONTRACT No. DNA 001-82-C-0197

APPROVED FOR PUBLIC RELEASE;
DISTRIBUTION UNLIMITED.

THIS WORK WAS SPONSORED BY THE DEFENSE NUCLEAR AGENCY
UNDER RDT&E RMSS CODE X322082469 Q78QAXHC00005 H2590D.

DTIC FILE COPY

Prepared for
Director
DEFENSE NUCLEAR AGENCY
Washington, DC 20305

DTIC
ELECTRONIC
S FEB 24 1984
A

84 01 20 087

Destroy this report when it is no longer
needed. Do not return to sender.

PLEASE NOTIFY THE DEFENSE NUCLEAR AGENCY,
ATTN: STTI, WASHINGTON, D.C. 20305, IF
YOUR ADDRESS IS INCORRECT, IF YOU WISH TO
BE DELETED FROM THE DISTRIBUTION LIST, OR
IF THE ADDRESSEE IS NO LONGER EMPLOYED BY
YOUR ORGANIZATION.



UNCLASSIFIED

SECURITY CLASSIFICATION OF THIS PAGE (When Data Entered)

REPORT DOCUMENTATION PAGE		READ INSTRUCTIONS BEFORE COMPLETING FORM
1. REPORT NUMBER DNA-TR-82-132	2. GOVT ACCESSION NO. AD-A138 290	3. RECIPIENT'S CATALOG NUMBER
4. TITLE (and Subtitle) REFRACTION DUE TO SHOCK WAVES		5. TYPE OF REPORT & PERIOD COVERED Technical Report
		6. PERFORMING ORG. REPORT NUMBER MRC-R-743
7. AUTHOR(s) Thomas J. Barrett Russell H. Christian		8. CONTRACT OR GRANT NUMBER(s) DNA 001-82-C-0197
		10. PROGRAM ELEMENT, PROJECT, TASK AREA & WORK UNIT NUMBERS Task Q78QAXHC-00005
9. PERFORMING ORGANIZATION NAME AND ADDRESS Mission Research Corporation P. O. Drawer 719 Santa Barbara, California 93102		12. REPORT DATE 1 March 1983
11. CONTROLLING OFFICE NAME AND ADDRESS Director Defense Nuclear Agency Washington, DC 20305		13. NUMBER OF PAGES 68
		15. SECURITY CLASS (of this report) UNCLASSIFIED
14. MONITORING AGENCY NAME & ADDRESS (if different from Controlling Office)		15a. DECLASSIFICATION/DOWNGRADING SCHEDULE N/A since UNCLASSIFIED
		16. DISTRIBUTION STATEMENT (of this Report) Approval for public release; distribution unlimited.
17. DISTRIBUTION STATEMENT (of the abstract entered in Block 20, if different from Report)		
18. SUPPLEMENTARY NOTES This work was sponsored by the Defense Nuclear Agency under RDT&E RMSS Code X322082469 Q78QAXHC00005 H2590D.		
19. KEY WORDS (Continue on reverse side if necessary and identify by block number) Refraction Blast Wave ROSCOE/NORSE Code		
20. ABSTRACT (Continue on reverse side if necessary and identify by block number) A simple procedure for estimating the refractive error produced by the density profile behind a nuclear blast wave is developed for use in radar system analysis codes such as ROSCOE/NORSE.		

DD FORM 1473
1 JAN 73

EDITION OF 1 NOV 65 IS OBSOLETE

UNCLASSIFIED
SECURITY CLASSIFICATION OF THIS PAGE (When Data Entered)

TABLE OF CONTENTS

<u>Section</u>		<u>Page</u>
1	INTRODUCTION	3
2	INDEX OF REFRACTION	5
3	SHOCK-INDUCED REFRACTIVE ERRORS	9
4	A MODULE TO PREDICT REFRACTION AND PRELIMINARY RESULTS	24
	REFERENCES	29
 <u>Appendix</u>		
I	ABSORPTION	31
	REFERENCES	42
II	SUBROUTINE LISTINGS	43



<input checked="" type="checkbox"/> CONFIDENTIAL <input type="checkbox"/> SECRET <input type="checkbox"/> RESTRICTED <input type="checkbox"/> CONFIDENTIAL	
Distribution/	
Availability Codes	
Dist	Avail and/or Special
A1	.

SECTION 1 INTRODUCTION

The modification of the index of refraction by a shock wave may produce refraction of electromagnetic signals, thus shock waves have the potential of introducing errors into radar system measurements of target locations. At high altitudes, i.e., in the ionosphere, refraction is determined by the amount of ionization present, but at low altitudes the increased electron-neutral collisional frequency causes the accompanying absorption to dominate any refraction so produced. Therefore any significant refraction produced at low altitude will be due to the changes in the atmospheric density and temperature. The atmospheric index of refraction as a function of these parameters is reviewed in Section 2.

In this approach to shock wave induced refraction it will be assumed that the given parameters include the actual target, burst and emitting source (radar) locations and that the resulting angular refractive error is the desired output. This is consistent with the current ROSCOE/NORSE code structure. It is also a more difficult problem to solve than predicting the arrival angle error of a specified ray, since the arrival angle of the ray that originates at the target is not a priori known. The errors expected are fortunately relatively small ($< 1^\circ$) thus a method of iteration beginning with the unrefracted ray, will be used. Section 3 presents these procedures for four possible cases, defined by the locations of the source and of the target relative to the shock front. The computer program and some preliminary results are described in Section 4. Program listings are included as an appendix.

Limits on when refraction due to spherically expanding shock waves need be considered have been generated. The early time limit to the importance of refractive effects is set by the cessation of absorptive effects. Exact values are of course sensitive to geometry, however the relatively strong dependence of ionization on temperature limits the temperature range of interest to between about 800° K for a long path to 1200° K to 1400° K for relatively short paths. This is further discussed in Appendix I where the absorption limit is discussed in detail. An absolute upper limit to the temperature of 1500° is suggested. The location of this temperature contour varies with time. At the shock front, the corresponding shock strength is about 25 psi overpressure, which occurs at a scaled range of $56(W_{KT})^{1/3}$ meters. The fireball however is significantly hotter than the shock and will move outward to almost twice this range.

The lower limit to when refraction need be predicted is a function of both the accuracy required and the location of the burst point relative to the sight path. For example, if an instantaneous refractive error of 1 milliradian is significant and if the shock wave becomes tangent to the sight path at about its mid point, then a density increase of 0.4 percent is sufficient and this corresponds to a shock overpressure of 0.03 psi, i.e., a relatively weak shock.

SECTION 2 INDEX OF REFRACTION

The index of refraction at any point is a function of both the amount of ionization present and of the density and temperature of the various neutral constituents. In analyzing refractive errors for propagation paths at low altitude, it is only necessary to consider the changes to the neutral constituents. This is because the absorption of electromagnetic energy is also proportional to the amount of ionization present and to the electron-neutral collisional frequency, which is proportional to pressure. Therefore at the lower altitudes high levels of absorption will occur on typical propagation paths that have even moderate amounts of refraction. This can be seen by comparing the angular deviation of the ray path, ψ in degrees, to the one-way absorption, A in dB. Reference 1 gives the approximate relation* for the case of spherically stratified ionization

$$\frac{\psi}{A} \approx \frac{10^7}{\nu r}, \quad \text{°/db} \quad (2-1)$$

where ν is the electron-neutral collision frequency (sec^{-1}) in the region and r is a characteristic dimension in (km). Using typical values, $\nu \approx 10^{11} \text{ sec}^{-1}$ and $r \approx \frac{1}{10} \text{ km}$, we obtain $\psi \approx 10^{-3}$ degree per db or 16 micro-radians per db, i.e., the absorption along a path that yields 1 milliradian deflection due to an ionization gradient will also yield 60 db of

* See for example Page 6-6 of Reference 1.

absorption. In the Appendix it is shown that when the temperature exceeds about 1000° K - 1500° K, then the quasi-equilibrium ionization resulting from delayed fission-product radiations will produce such high levels of absorption. Therefore when predicting refraction caused by a shock wave it is only necessary to consider the impact of density and temperature changes on the index of refraction, and only for temperatures below 1500°K.

A best fit to the data on the atmospheric refractive index at radio frequencies was determined at NBS and reported in Reference 2 to be (their Equation 7)

$$N = (n-1)10^6 = 77.6 \frac{P}{T} - 6 \frac{e}{T} + 3.75 \times 10^5 \frac{e}{T^2} \quad (2-2)$$

where P is the total pressure, in millibars, T is the absolute temperature, in °K, and e is the partial pressure of water vapor, in millibars. A form that contains the wavelength dependence can be used to show that this dependence is negligible at radio frequencies. This form is as given by Allen (Reference 3) at STP as

$$(n-1) \times 10^6 = 64.328 + \frac{29498.1}{146 - (\frac{1}{\lambda})^2} + \frac{255.4}{41 - (\frac{1}{\lambda})^2}, \text{ at } 15^\circ\text{C} \quad (2-3)$$

where λ is the vacuum wavelength in microns. Since we are not interested in wavelengths less than one mm or 10^3 microns, the corrections are always negligible and this reduces to $(n-1) \times 10^6 = 272.6$, consistent with Equation 2-2 above.

It is convenient to simplify Equation 2-2. We introduce the relative partial pressure of water vapor, $\epsilon' = \epsilon/p$. The gas law allows

p/T to be replaced by the density, ρ , in gm/cm^3 , which then can be factored out. Following Reference 3, we can also combine the second term with the third term with only small error for the temperature range of interest - especially since the ambient value of e' is highly variable.

$$N = (n-1)10^6 = 2.2 \times 10^5 \rho \left(1 + 4.8 \times 10^3 \frac{e'}{T} \right) \quad (2-4a)$$

or

$$n = 1 + 0.22 \rho \left(1 + 4.8 \times 10^3 \frac{e'}{T} \right) . \quad (2-4b)$$

Later it will be convenient to consider the ratio of the indices of refraction across a shock front. Using the subscripts o and s to signify the ambient and shocked conditions, this ratio is

$$\frac{n_s}{n_o} = \frac{1 + 0.22 \rho_s \left(1 + 4.8 \times 10^3 \frac{e'}{T_s} \right)}{1 + 0.22 \rho_o \left(1 + 4.8 \times 10^3 \frac{e'}{T_o} \right)} \quad (2-5)$$

which can be closely approximated by

$$\begin{aligned} \frac{n_s}{n_o} &\approx \left[1 + 0.22 \rho_s \left(1 + 4.8 \times 10^3 \frac{e'}{T_s} \right) \right] \left[1 - 0.22 \rho_o \left(1 + 4.8 \times 10^3 \frac{e'}{T_o} \right) \right] \\ &\approx 1 + 0.22 \rho_o \left[\left(\frac{\rho_s}{\rho_o} - 1 \right) + 4.8 \times 10^3 \frac{e'}{T_o} \left(\frac{\rho_s}{\rho_o} \cdot \frac{T_o}{T_s} - 1 \right) \right] . \end{aligned} \quad (2-6)$$

In this form we see that an accurate knowledge of the water vapor content is usually not important. In much of the range of interest the compression ratio is about 40% greater than the shock temperature ratio.

Using an ambient temperature of 288° K the second term in the bracket becomes 6.7 e'. Typical values of e' are less than 0.03, yielding a value of 0.2 or less, to be compared with the shock overdensity ratio, $(\rho_s/\rho_0-1) \equiv (\mu-1)$, which is generally much greater.

For discussion purposes, it is convenient to use an ambient density of 10^{-3} g/cm³ (and a value corresponding to an altitude of about 6000 ft above sea level) and a relatively high value of water vapor partial pressure of 3% (corresponding to saturated air at about 25° C). Equation 2.6 then becomes

$$\frac{\eta_s}{\eta_0} = 1 + 2.2 \times 10^{-4} \left[(\mu-1) + \frac{1}{2} \left(\mu \frac{T_0}{T_s} - 1 \right) \right] . \quad (2-7)$$

It is shown in the Appendix that if the shock temperature exceeds about 4 times ambient temperature then absorption is the dominant process. The corresponding compression ratio, $\mu = \frac{\rho_s}{\rho_0}$, is 4.7. Inserting these values into Equation 2-7 yields an upper limiting value of

$$\frac{\eta_s}{\eta_0} = 1 + 2.2 \times 10^{-4} \left[3.7 + \frac{1}{2} \left(\frac{4.7}{4} - 1 \right) \right] = 1 + 8.3 \times 10^{-4} \quad (2-8)$$

SECTION 3 SHOCK-INDUCED REFRACTIVE ERRORS

The geometry of the shock wave related refraction problem is shown in Figures 1 and 2. The ambient (external) atmosphere is assumed to be uniform and the shock wave is assumed to be spherical. Therefore the source, target and burst points define the plane of these figures. There is no refraction out of this plane. Figure 1 shows the larger view of this plane. A source (e.g., radar) is located at the bottom of the figure, tracking a target at the top which is moving to the left. A burst occurs at a range R_B from the source. The angle at the source between the sight lines to the burst and to the real location of the target is θ_1 . A shock wave is expanding from the burst, at a radius S_R . The density increase within the shock wave produces an increase in the local index of refraction. Refractive effects will occur only after the target passes behind the shock front, i.e., not until after it passes point T_0 . When viewed through the shocked region the apparent target location T' will be to the right (in this figure) of the real location, T . As the shock wave intercepts the line of sight there will be a portion of the trajectory that is not visible. Of course, in the general case the current shock location could be beyond either the target or source location or beyond both.

Figure 2 illustrates a possible propagation path within the shocked region. The insert at the top of the figure shows a possible radial profile of density. This profile, including the current shock radius is assumed to be given. For example it may be obtained from the Nuclear Blast Standard (1 KT) (Reference 4), the LAMB code (which includes

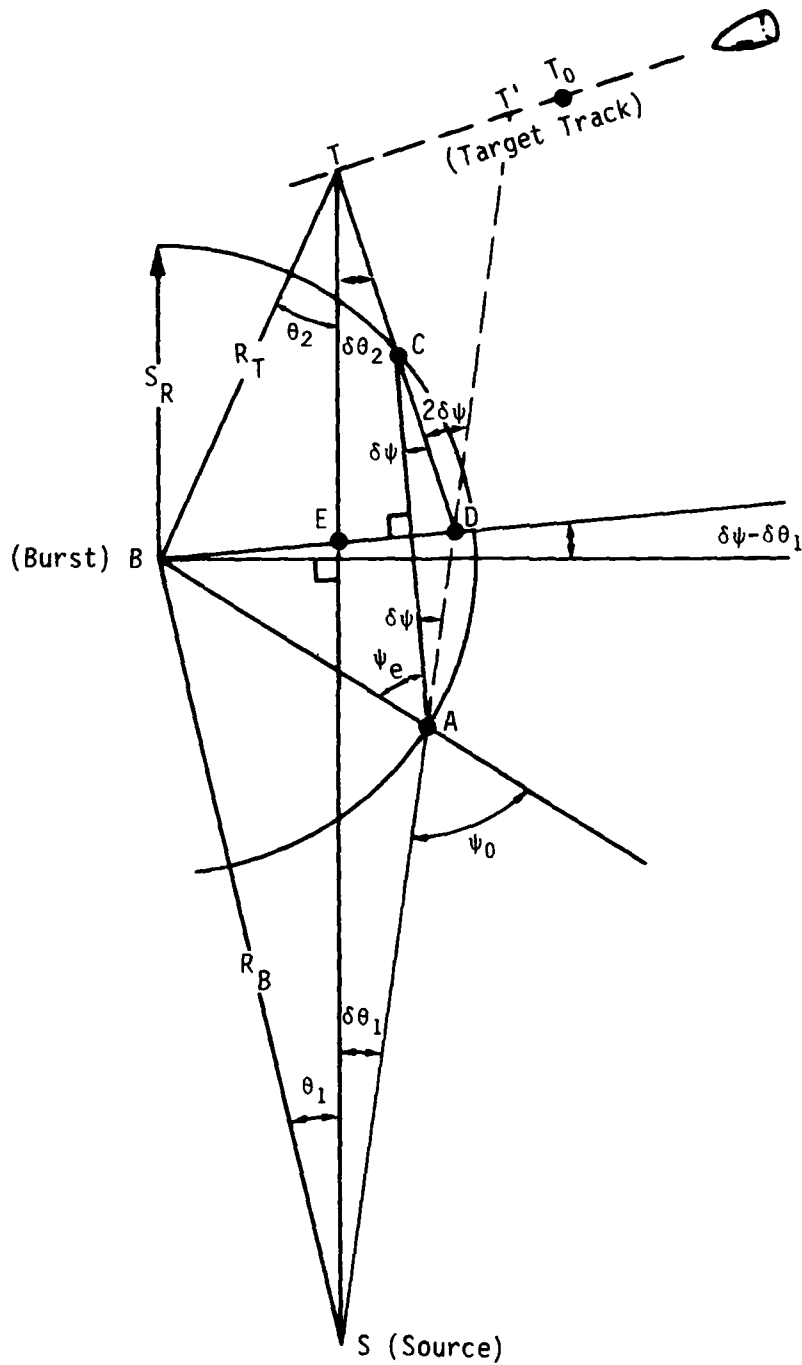


Figure 1. Geometric definitions outside the shock.

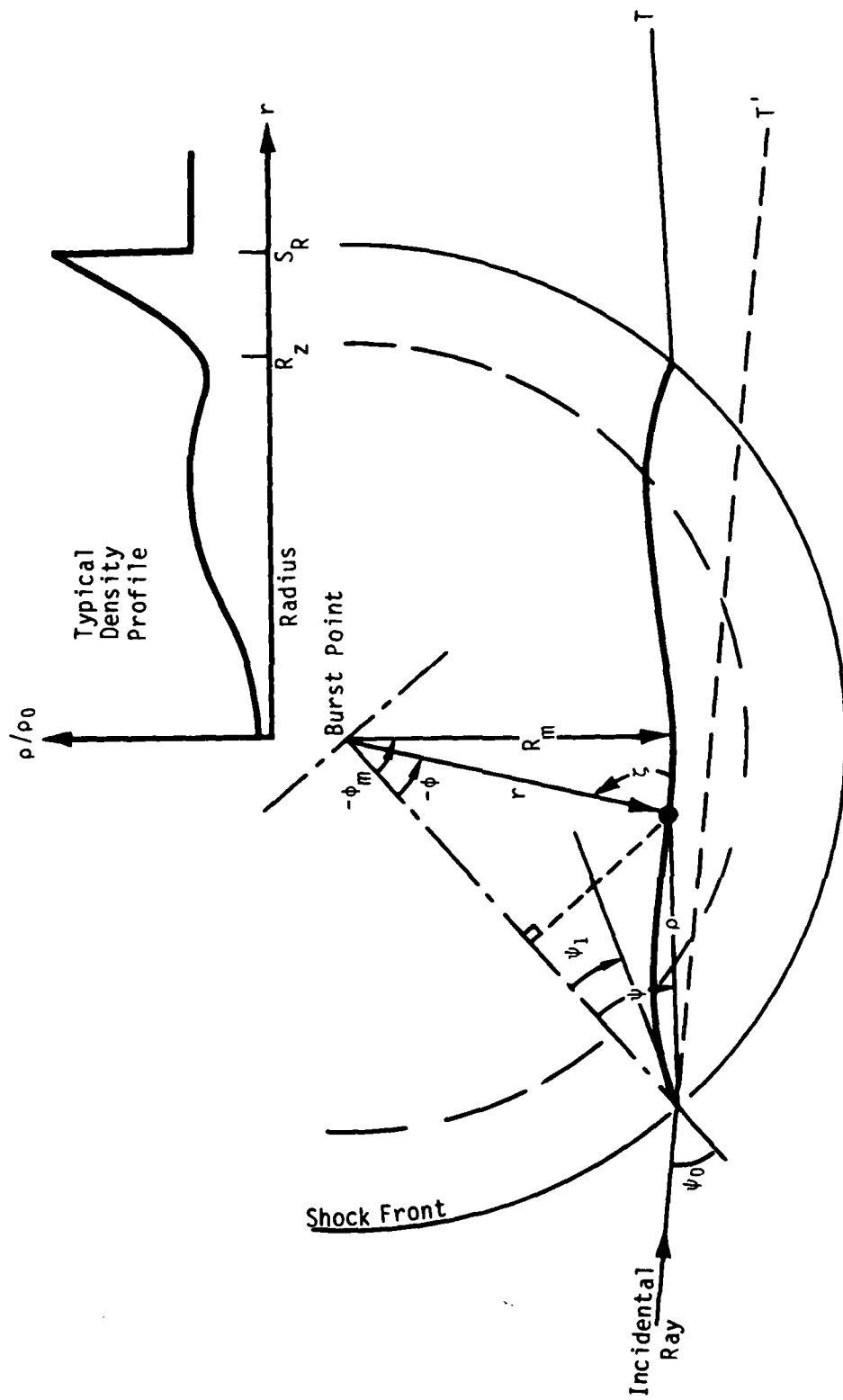


Figure 2. Geometric definitions for refraction within a spherically stratified region.

the 1 KT standard) or other simple fits to the well known blast wave data. In Figure 2 the reference axis has been chosen along the radial between the burst point and the entry point of the ray path. Note that the location of this entry point, and thus also the angle ψ_0 are to be determined, and when known represents the solution of the problem.

The location of the target, labeled T, may be anywhere along the path, including inside the shock. The apparent location, T', will be along the dashed extension of the incident ray, at different range. The propagation path starts from S at the angle $(\theta_1 + \delta\theta_1)$ and enters the shock at point A where it makes the angle ψ_0 with a radial from the burst point. The actual ray to the target is refracted towards this radial through an angle $\delta\psi$. When both the radar and target are outside the shocked region the ray path exits the shock at point C where it is refracted away from the radial through C by the same angle $\delta\psi$, and arrives at the target location at an angle $\delta\theta_2$ off of the line S-T. In this case of spherical symmetry it is possible to replace the actual curved path by a straight line connecting the entry and exit points. This is equivalent to approximating the radially varying value of the index of refraction by some 'effective' value, \bar{n} , yet to be defined.

REFRACTION IN A SPHERICALLY STRATIFIED REGION

Referring to Figure 2, the polar coordinates of an arbitrary point along the ray path interior to the shock as measured from the burst point are (r, ϕ) , and as measured in polar coordinates from the entry point are (ρ, ψ) . The angle between the vector r and the local direction of the ray path is ζ . Note from the geometry of these definitions that

$$\rho \sin \psi = -r \sin \phi$$

and

$$\rho \cos \psi = S_R - r \cos \phi$$

thus

$$\psi = \tan^{-1} \left(\frac{r \sin \phi}{S_R - r \cos \phi} \right) . \quad (3-1)$$

The change in ray direction upon shock entry (and when appropriate upon exit) is obtained from Snell's law. Note that at entry point $\psi_1 \equiv \zeta_s$. Thus

$$n_0 \sin \psi_0 = n_s \sin \psi_1 = n_s \sin \zeta_s . \quad (3-2)$$

The solution for the ray path within a spherically stratified region has been given by Archer (References 5 and 6). The form of Snell's law for a spherically stratified medium is

$$r n(r) \sin \zeta = K \quad (3-3)$$

The radial variation of n is obtained by substituting the given radial variations of density, $\rho(r)$, and of temperature, $T(r)$, into equation (2-4b) of the previous section. The constant K may be defined by values either upon entry or at the point of closest approach where, $\zeta = \pi/2$ and $r = R_m$. Combining equations 3-2 and 3-3 provides a relation between R_m and the (as yet unknown) angle of incidence outside the shock, yields

$$K = r n(r) \sin \zeta \quad (3-4a)$$

$$= R_m n(R_m) \quad (3-4b)$$

$$= S_R n_s \sin \zeta_s = S_R n_s \sin \psi_1 \quad (3-4c)$$

$$= S_R n_0 \sin \psi_0 \quad (3-4d)$$

The differential equation of the ray path within the shocked region is

$$d\phi = \frac{\pm K dr}{r \sqrt{r^2 n^2(r) - K^2}} \quad (3-5)$$

The integral of this equation between two points (r_1, ϕ_1) and (r_2, ϕ_2) provides the angle $\phi = \phi_2 - \phi_1$ between these points, i.e.,

$$\phi = \oint_{r_1}^{r_2} \frac{K dr}{r \sqrt{r^2 n^2(r) - K^2}} \quad (3-6)$$

where we have used the symbol \oint to indicate the integral is to be taken along a specific path and not just between the radial points r_1 and r_2 . Specifically, for paths which pass through the point of closest approach this integral runs from r_1 to R_m to r_2 . In the following, the point r_1 is either the known location of the source when the source is within the shock or the entry point of the ray path when the source is outside. Note that while the radius to that entry point is known (i.e., S_p) its angular position is not known. Similarly r_2 refers to either the target location or the exit point of the ray path.

Unfortunately the constant K in equation 6 contains R_m which depends on the ray path, or equivalently the angle ψ_0 which depends on the entry point. Therefore it is necessary to solve the set of equations iteratively. Fortunately, we are interested only when the refractive error is small, thus the undeviated path provides a first estimate of R_m or ψ_0 . From Figure 1 this can be seen to be

$$R_m \approx R_B \sin \theta_1 \quad (3-7)$$

Using this value of r , a density and temperature are obtained from the given shock wave profile. These are then used in equation 2-4b to obtain the local index of refraction. This together with the radius then provides the initial estimate of K .

BEARING ERROR PREDICTIONS

There are four possible geometric situations that may occur depending on the relative location of the shock to the source and to the target. Each requires a slightly different method of solution, although the principle remains the same. Using the assumption that the refractive error is small, K as obtained above is used to determine a first estimate of the angular extent of the ray path interior to the shock, ϕ . In three of these cases, geometric considerations then provide an estimate of the shock front entry or exit angle, which provides a second estimate of K and leads to a situation that may be iterated. In the fourth case, which we shall discuss first, the iteration is on the location of R_m since the shock front is never reached.

Source and Target Both Within the Shocked Zone

In this case the angular extent, ϕ , must be equal to the angle at the burst point between the radii to the source and the target, i.e.,

$$\phi = \pi - (\theta_1 + \theta_2) \quad (3-8)$$

The end points of the integral are also determined by geometry, thus the only available parameter is K , or equivalently the location of the minimum radius to the propagation path. Given that parameter the initial direction of the ray is obtained from equation 3-4a. The refractive error is then the difference between this angle and θ_1 , i.e.,

$$\delta\theta_1 = \zeta(R_B) - \theta_1 \quad (3-9a)$$

$$= \sin^{-1} \left[\frac{K}{R_B n(R_B)} \right] - \theta_1 \quad (3-9b)$$

An estimate of the correction to K necessary to make the calculated value of ϕ agree with the geometric value may be obtained by differentiating equation 3-6 w.r.t K.

$$\begin{aligned} \frac{d\phi}{dk} &= \frac{d}{dk} \int_{r_1}^{r_2} \frac{K dr}{r \sqrt{r^2 n^2(r) - K^2}} + F(r_2, K) \frac{dr_2}{dk} - F(r_1, K) \frac{dr_1}{dk} \\ &= \int_{r_1}^{r_2} \left(1 + \frac{K^2}{r^2 n^2(r) - K^2} \right) \frac{dr}{r \sqrt{r^2 n^2(r) - K^2}} + 0 - 0 \\ &= \int_{r_1}^{r_2} \frac{r n^2(r) dr}{(r^2 n^2(r) - K^2)^{3/2}} \end{aligned} \quad (3-10)$$

Source Outside and Target Inside

This situation is illustrated in Figure 3. The initial estimate of ϕ is based on K as obtained from R_m , equation 3-4b. This then defines a revised entry point and thus a new value for ψ_0 from geometry, i.e., two sides (R_B and S_R) and the included angle ($\theta_3 - \phi$) of the triangle S-B-O are known. The revised value of K, obtained from equation 3-4d, is then used to recalculate ϕ . The process is iterated for a consistent set (ϕ, ψ_0). The refractive error, by geometry is then

$$\delta\theta_1 = \psi_0 - \theta_1 - (\theta_3 - \phi) = \psi_0 + \theta_2 - \pi + \phi \quad (3-11)$$

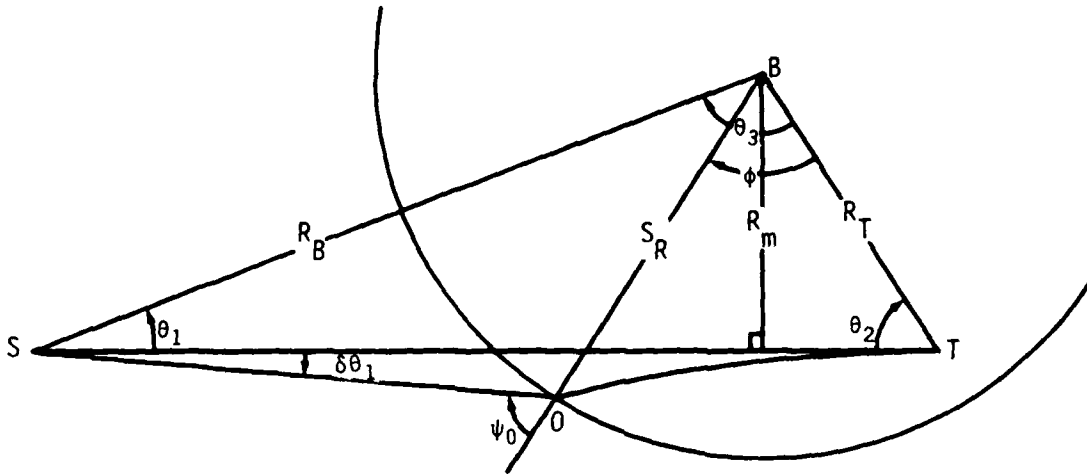


Figure 3. Source outside and target inside the shocked region.

Note that the curved nature of the path interior to the shock does not enter directly.

Source Inside, Target Outside

This is essentially the inverse of the previous case with one major difference, since the refractive error occurs on the curved portion of the path which extends to the source. The method of solution is essentially the same, except that once the consistent set (ϕ, ψ_0) is obtained the corresponding value of K is used in equation 3-4a to obtain the instantaneous ray path angle ζ at the radius R_B . The refractive error is then

$$\delta\theta_1 = \zeta(R_B) - \theta_1$$

which is the same as equation 3-9a.

Target and Source Both Outside

When the propagation path completely traverses the shocked region as depicted in Figures 1 and 2, then the radial from B to D will be perpendicular to this path and the angle ψ_0 (or B-A-C) is the complement of the angle ϕ_m (or A-B-D), where ϕ_m is defined as one-half the total angular extent of the ray path inside the shock, i.e.,

$$\phi_m = \int_{S_R}^R \frac{K dr}{r \sqrt{r^2 n^2(r) - K^2}} \quad (3-12)$$

The effective value of the index of refraction which corresponds to a straight line path inside the shock, is

$$n_e \approx n_0 \sin \psi_0 / \sin \psi_e = n_0 \sin \psi_0 / \cos \phi_m \quad (3-13)$$

Consider the triangles formed by the unrefracted extension of the external ray paths. From the small triangle the angle between lines S-A-D and D-C-T is $2\delta\psi$. From the large triangle (S,T,D) that angle is $\delta\theta_1 + \delta\theta_2$. Thus

$$\delta\theta_1 + \delta\theta_2 = 2(\psi_0 - \psi_e) = 2\delta\psi \quad (3-14)$$

The angle between the radial BD and the radial that is perpendicular to ST can be seen to be $(\delta\psi - \delta\theta_1)$ which is also $\frac{1}{2}(\delta\theta_2 - \delta\theta_1)$.

Applying the law of sines to the triangles S-E-D and D-E-T yields

$$(R_1 + d) \sin \delta\theta_1 = \ell \sin(90 - \delta\psi) = (R_2 - d) \sin \delta\theta_2, \quad (3-15)$$

where

$$R_1 = R_B \cos \theta_1$$

$$R_2 = R_T \cos \theta_2$$

$$d = R_B \sin \theta_1 \cdot \tan\left(\frac{\delta\theta_2 - \delta\theta_1}{2}\right) .$$

$\delta\theta_1$ and $\delta\theta_2$ are small angles, thus the sines in equation 3-15 may be approximated by the angles, yielding

$$(R_1 + d) \delta\theta_1 \approx (R_2 - d) \delta\theta_2 .$$

Using this in Equation 3-14 to eliminate $\delta\theta_2$ yields

$$\left(1 + \frac{R_1 + d}{R_2 - d}\right) \delta\theta_1 = 2\delta\psi .$$

d can also be neglected, being much smaller than either R_1 or R_2 , yielding

$$\left(1 + \frac{R_1}{R_2}\right) \delta\theta_1 = 2\delta\psi . \quad (3-16)$$

A relation between the viewing angle, $\theta_1 + \delta\theta_1$ and the angle of incidence, ψ , of the ray SA at the shock front is obtained by applying the law of sines to triangle S-B-A.

$$\frac{\sin(\theta_1 + \delta\theta_1)}{S_R} = \frac{\sin(180 - \psi_0)}{R_B} = \frac{\sin \psi_0}{R_B} \quad (3-17)$$

We now apply Snell's law in the form

$$n_0 \sin \psi_0 = n_e \sin (\psi_0 - \delta\psi) \quad (3-18)$$

where n_e is the "effective" value behind the shock. Expanding the left side of Equations 3-18 and rearranging yields

$$\tan \psi_0 = \frac{\sin \delta\psi}{\cos \delta\psi - n_0/n_e} \quad (3-19)$$

To eliminate ψ_0 we rewrite $\sin \psi_0$ in Equation 3-17 in terms of the tangent ψ_0 and substitute from Equation 3-19, thus

$$\begin{aligned} \frac{R_B}{S_R} \sin (\theta_1 + \delta\theta_1) &= \sin \psi_0 = \frac{\tan \psi_0}{\sqrt{\tan^2 \psi_0 + 1}} \\ &= \frac{\sin \delta\psi}{\sqrt{\sin^2 \delta\psi + \cos^2 \delta\psi - 2 (n_0/n_e) \cos \delta\psi + (n_0/n_e)^2}} \\ &= \frac{\sin \delta\psi}{\sqrt{\left(1 - \frac{n_0}{n_e}\right)^2 + 2 \frac{n_0}{n_e} (1 - \cos \delta\psi)}} \end{aligned} \quad (3-20)$$

Equation 3-16 is used to eliminate $\delta\psi$ yielding an equation containing $\delta\theta_1$ and known quantities,

$$\frac{R_B}{S_R} \sin (\theta_1 + \delta\theta_1) = \frac{\sin \left(\frac{R_1 + R_2}{2R_2} \delta\theta_1 \right)}{\sqrt{\left(1 - \frac{n_0}{n_e}\right)^2 + 2 \frac{n_0}{n_e} \left[1 - \cos \left(\frac{R_1 + R_2}{2R_2} \delta\theta_1 \right)\right]}} \quad (3-21)$$

We expect $\delta\theta_1$ to be a small angle and do not expect the factor $(\frac{R_1+R_2}{2R_2})$ to prevent a small angle approximation, then

$$\frac{R_B}{S_R} (\sin \theta_1 + \delta\theta_1 \cos \theta_1) = \frac{(\frac{R_1+R_2}{2R_2}) \delta\theta_1}{\sqrt{(1 - \frac{n_0}{n_e})^2 + \frac{n_0}{n_e} [(\frac{R_1+R_2}{2R_2}) \delta\theta_1]^2}} \quad (3-22)$$

From Equation 2-8 we expect the first term in the square root to be of the order of, but less than $(8.3 \times 10^{-4})^2$. This generally will be smaller than the second term whenever refraction exceeds a few milliradians, therefore as a first estimate we neglect the first term, yielding

$$\frac{R_B}{S_R} (\sin \theta_1 + \delta\theta_1 \cos \theta_1) = \sqrt{\frac{n_e}{n_0}} \quad (3-23)$$

or

$$\delta\theta_1 \approx \frac{\frac{S_R}{R_B} \sqrt{\frac{n_e}{n_0}} - \sin \theta_1}{\cos \theta_1} \quad (3-24)$$

REAPPEARANCE

As the line of sight to the target passes behind the shock front the target will disappear (ignoring diffraction) and will not reappear until the external rays S-A and C-T₂ are tangent to the shock, i.e., the angle of incidence, ψ_0 is 90°. From equation 3-18 and 3-16,

$$\begin{aligned} \frac{n_0}{n_e} &= \sin \left(\frac{\pi}{2} - \delta\psi \right) = \cos \delta\psi \\ &= \cos \left(\frac{R_1+R_2}{2R_2} \delta\theta_1 \right) \end{aligned} \quad (3-25)$$

Again in the small angle approximation

$$\frac{n_0}{n_e} = 1 - \frac{1}{2} \left[\frac{R_1 + R_2}{2R_2} \delta\theta_1 \right]^2 \quad (3-26)$$

Inverting,

$$\delta\theta_1 = \frac{2R_2}{R_1 + R_2} \sqrt{2 \left(1 - \frac{n_0}{n_e} \right)} \quad (3-27)$$

Substituting the index of refraction ratio from equation (2-6) gives

$$\delta\theta_1 = \frac{2R_2}{R_1 + R_2} \sqrt{2 (.22) \rho_0 [(\mu - 1) + 4.8 \times 10^3 \frac{\epsilon'}{T_0} \left(\mu \frac{T_0}{T_s} - 1 \right)]}, \quad (3-28)$$

for $\rho_0 \approx 10^{-3}$

$$\delta\theta_1 = \left(\frac{2R_2}{R_1 + R_2} \right) (.02) [(\mu - 1) + 4.8 \times 10^3 \frac{\epsilon'}{T_0} \left(\mu \frac{T_0}{T_s} - 1 \right)]^{1/2}, \quad (3-29)$$

when the shock first becomes transparent at $T_s \approx 4 T_0$ and $\mu = 4.7$, the square root term yields about a factor of 2 thus the refraction error will be about 40 milliradians times the factor involving the relative locations (which is usually of the order of unity).

If we define the minimum value of interest for $\delta\theta_1$ we can then determine the minimum shock strength and therefore the maximum shock radius of interest. We can convert equation 3-29 into terms of the relative shock overpressure, $\pi = \frac{p}{p_0} - 1$, using the Hugoniot relation

$$\mu = \frac{7 + 6 \pi}{7 + \pi}$$

and the ideal gas law

$$\frac{T_0}{T_s} = \frac{p_0}{p} \cdot \frac{\rho}{\rho_0} = \frac{\mu}{1+\pi} .$$

Substitution of these into equation (3-29) yields

$$\delta\theta_1 = \left(\frac{2R_2}{R_1+R_2} \right) (.02) \left[\frac{5\pi}{7+\pi} + \frac{16 \epsilon'}{(7+\pi)^2} \left(21\pi - \frac{\pi^3}{1+\pi} \right) \right]^{1/2} \quad (3-30)$$

which for weak shocks reduces to

$$\delta\theta_1 = \left(\frac{2R_2}{R_1+R_2} \right) (.02) \left[\frac{5\pi}{7} (1+10\epsilon') \right]^{1/2} , \pi \ll 1 \quad (3-31)$$

For example, to produce the above estimate to, say, 1 milliradian, would require that the factor within the square root be only $\frac{1}{400}$ which occurs at about an overpressure of about 0.03 psi, i.e., in the far field of the shock wave.

SECTION 4
A MODULE TO PREDICT REFRACTION
AND PRELIMINARY RESULTS

A set of subroutines was prepared with the intent that an appropriate subset could easily be adopted into larger programs. These subroutines and their functions are described in the following paragraphs.

Program BLAST and subroutine GETINPUT provide our stand-alone driver that would be replaced by a calling procedure within the larger program. Inputs that are expected, units used, and where appropriate default values, are:

- 1) RHOA = Ambient air density (gm/cm³, default = 1.225×10^{-3})
- 2) TEMPA = Ambient air temperature (°K, default = 288)
- 3) WATER = Relative partial water vapor pressure (default = .01)
- 4) W = Effective blast yield (kilotons)
- 5) TIME = Time of interest after burst (sec)
- 6) RBS = Actual range between source and burst (cm)
- 7) RTS = Actual range between source and target (cm)
- 8) THETA1 = Actual angle between RBS and RTS (radians)

In the stand-alone version these are obtained via a common block from subroutine GETINPUT in which the default values are stored.

SUBROUTINE REFRACT

Subroutine REFRACT is the heart of the calculational procedure. The first step is to scale ranges and time to equivalent one kiloton

values so that the shock location (i.e., radius) and density profile data can be obtained from the AFWL Nuclear Blast Standard (1 KT) (Reference 4) via a call to DENSITY. Then a set of tests is performed to determine the relative locations of the source and the target relative to the shock front and whether or not the LOS extends to the point of closest approach (RMIN) of the LOS to the burst. These tests define the approximation procedures and the integration limits.

The primary output provided is the refractive error, in radians, in the plane formed by the burst point, target and source: that is, the increase in the angle THETA1 caused by the refraction of the ray path in passing through the density profile of the blast wave. Additional outputs that are available include PSIO, the angle of incident at the shock front (when the source is outside); relative locations of target or source with respect to the shock, and the interior angle ϕ ; and \bar{n} , the effective index of refraction (when both target and source are outside).

SUBROUTINE ETA

Subroutine ETA returns the index of refraction within the shocked region according to Equation 2-4b. The input is the scaled radial dimension of the point of interest. This subroutine then calls the 1 KT blast model to obtain the overdensity via the common block /WFRT/. A temperature is needed in Equation 2-4b as part of the water vapor correction. The 1 KT blast model does not provide a temperature or internal energy profile behind the blast wave. Although a temperature could be obtained from the overpressure profile and the equation of state through an iteration procedure, a simple approximation has been used instead. The temperature is estimated by assuming a gamma law expansion (at $\gamma = 1.4$) from the current shock front density, but limited to be at least ambient temperature. This is rationalized as being sufficient since the shock

temperature does not exceed 1200° K, thus any error in the temperature will probably be less than the uncertainty in the partial pressure of the water vapor.

SUBROUTINE INTEGRT

This subroutine performs the integration of Equation 3-6 to provide the angle ϕ between radial limits supplied to it by subroutine REFRACT. The procedure used is to subdivide this interval into steps within which the value of eta is essentially constant. Equation 3-6 can then be integrated analytically to give the increment, $\Delta\phi$, over each step, Δr , i.e.,

$$(\Delta\phi)_i = \frac{K}{n_i} \int_{r_i}^{r_i+\Delta r} \frac{dr}{r\sqrt{r^2 - (K/n_i)^2}} = \cos^{-1} \left(\frac{K}{n_i r_i} \right) - \cos^{-1} \left(\frac{K}{n_i (r_i + \Delta r)} \right)$$

where n_i is the value of the index of refraction at the center of the i th interval. The approximate number of steps to be taken is specified by a data statement as NUM, however the step size can be decreased or increased internally based on a test of the relative change of the index of refraction within each step.

The calling sequence for this subroutine expects

- RS = First integration limit of scaled radius
- RM = Second integration limit
- CK = Constant K of equation 3-6
- ETANEW = Value of eta at starting point of integration
- DPDK = A trigger value which causes a calculation of $\frac{d\phi}{dK}$ when positive or zero, but skips this calculation when set negative

Upon return, in addition to providing the values of ϕ and when requested $\frac{d\phi}{dk}$, the subroutine stores the most recent values of n_i in ETANEW for use in the second integration when needed.

SUBROUTINES DENSITY AND AIRPT

Subroutine DENSITY contains only those portions of the 1 KT blast standard that are required for the refraction prediction. These were extracted from Reference 4 and are carried as a separate routine so that when the more complete set of blast subroutines is used elsewhere within a larger code, this subroutine can be deleted and that set used. An initial call to DENSITY (TIME) at each time of interest sets the following parameters.

PRAD = Shock front radius (cm)
OPPK = Peak overpressure, at PRAD (dyne/cm²)
ODPK = Peak overdensity, at PRAD (gm/cm³)
RDZ = Radius at which overdensity passes through zero (cm)
TEMPK = Shock front temperature (*K)

Subsequent calls at the same time use entry DENS(RAD) and obtain ODR, the overdensity at the specified radius, RAD. Outputs from DENSITY are transferred via the common block /WFRT/. Subroutine DENSITY requires the air equation of state to calculate ODPK, from the prediction value of OPPK.

The DOAN-NICKLE equation of state of air as given in subroutine AIRPT(E,R,G,P,T) of the MDAC version of LAMB has been used, since it includes the temperature and pressure thus providing TEMPK. This subroutine appears to include the subroutine AIR(E,R,G) of the 1 KT standard, which may be accessed through an entry call.

TYPICAL RESULTS

These subroutines have been exercised for the several conceivable types of sight paths, depending on the relative location of the radar target, shock wave and point of closest approach to the burst point of the sight path. For those case in which absorption dominates or where the shock is not intersected a message to that effect is produced without the prediction of refraction. Table 1 describes eight possible sight paths through the shock wave from a one kiloton burst at one second and lists the calculated refractive error.

Table 1. Sight path parameters and results.

Case	RBS	RTS	θ_1	$\delta\theta_1$
	cm	cm	radians	milliradians
1	1.3E5	1E5	.1	8.4E-4
2	1.3E5	1.6E5	.15	2.9E-2
3	1.3E4	2E4	.7	2.5E-4
4	3E4	5E4	.72	-6.0E-5
5	2.5E4	3E4	1.9	658.(?)
6	4E4	2E5	.7	0.136
7	3E4	1.5E5	2.1	-1058.(?)
8	1.5E5	2.5E5	.22	16 to 104(*)

(?) These values are abnormally large; indicating that the "small derivation" approximation is invalid but do show that refraction will be an extremely severe problem.

(*) This case did not converge but oscillated between these values, again indicating a serious refractive error.

REFERENCES

1. Knapp, W. S. and K. Schwartz, "Aids for the Study of Electromagnetic Blackout," DNA 3499H, GE TEMPO, February 1975.
2. Smith, E. K., Jr., and S. Weintraub, "The Constants in the Equation for Atmospheric Refractive Index at Radio Frequencies," J. Res. NBS, 50, pp 39-41, January 1953.
3. Allen, C. W., Astrophysical Quantities, 3rd Edition, University of London, The Athlone Press (1976).
4. Needham, C. E., M. L. Havens, and C. S. Knauth, " Nuclear Blast Standard (1 KT)," AFWL-TR-73-55 (Rev), Air Force Weapons Laboratory, April 1975.
5. Archer, D. H., "Refraction of Electromagnetic Waves in an Absorbing Region," RM59TMP-27, GE TEMPO, 10 June 1959.
6. Archer, D. H., "Position and Rate Errors Due to Refraction Through Ionized Regions," RM59TMP-26, GE TEMPO, 31 December 1959.

APPENDIX I ABSORPTION

When the electron concentration within a shock wave is sufficiently high, the absorption of electromagnetic waves becomes so great that refraction effects can be ignored. Here we will generate estimates of the conditions at which such circumstances occur and identify those cases wherein refraction might be important. Except where noted, the basic equation used below are from The Aids for the Study of Electromagnetic Blackout (Reference 1).

The differential absorption of an electromagnetic wave of angular frequency, ω (radians/sec), can be expressed as

$$A_b = \frac{46 \text{ gv}}{(g\nu)^2 + (h\omega)^2} N_e, \quad \text{db/m} \quad (I-1)$$

where N_e is the local electron concentration (e/cm^3) and ν is the electron collision frequency (sec^{-1}). At altitudes below about 100 km the collision frequency of importance is that with neutral particles, which is

$$\nu = 1.7 \times 10^5 p, \quad \text{sec}^{-1} \quad (I-2)$$

where p is the local air pressure ($dynes/cm^2$). At sea level the ambient pressure is $p_0 = 10^6 \text{ dyne/cm}^2$ hence $\nu_0 = 1.7 \times 10^{11} \text{ sec}^{-1}$ which corresponds to an operating frequency, $f = \frac{\omega}{2\pi} = \frac{\nu}{2\pi} = 2.7 \times 10^{10} = 27 \text{ Ghz}$. The operating frequencies of interest may be on either side of the collision frequency.

The factors g and h in Equation I-1 above are correction factors to account for the velocity dependence of electron-neutral collisions. For representative calculations values of these factors, as obtained from graphs in Reference 1, are given in Table I-1 below

Table I-1. Typical values of g and h .

	g	h
$\omega \ll \nu$	0.6 to 0.65	> 1.7
$\omega \approx .4 \nu$	0.75	1.3
$\omega > \nu$	1	1

For $\omega \ll \nu$ absorption is independent of the operating frequency and Equation (I-1) can be written

$$Ab = 75 \frac{N_e}{\nu}, \quad \omega \ll \nu, \quad \text{db/m} \quad (\text{I-3})$$

Using the sea level, ambient value of ν this becomes

$$Ab = 4.5 \times 10^{-10} N_e, \quad f \ll 27 \text{ Ghz}, \quad \text{db/m} \quad (\text{I-3a})$$

At 10 Ghz Equation (I-1) becomes

$$Ab = \frac{61 N_e}{\nu \left[1 + \left(.64 \frac{P_0}{P} \right)^2 \right]}, \quad f = 10 \text{ Ghz}, \quad \text{db/m} \quad (\text{I-4})$$

Using sea-level conditions in Equation I-4 yields

$$A_b = 2.5 \times 10^{-10} N_e , \quad \text{db/m} . \quad (\text{I-4a})$$

Note that the second factor in the denominator of Equation I-4 reduced the absorption by about 40%, but will contribute much less in a strongly shocked region.

For frequencies well above the collision frequency, i.e., millimeter waves, Equation (I-1) becomes

$$A_b = 46 \frac{\nu}{\omega^2} N_e , \quad \omega \gg \nu \quad \text{db/m} \quad (\text{I-5})$$

Probably the minimum path length through the shocked region that is ever of interest will be a few tens of meters. Normally the path will be much longer, i.e., one-hundred or more meters. Equation I-3a indicates that an electron concentration of 10^9 e/cm^3 would yield about 10 db (one-way) or 20 db (two-way) absorption over a 20 meter path. Equation I-4a would require a 40 meter path or twice the electron concentration. Similarly, Equation I-5 indicates that 10^{10} e/cm^3 will produce high levels of absorption at a frequency of 95 Ghz. One thus concludes that if the electron concentration exceeds 10^9 , or perhaps 10^{10} depending on geometry and operating frequency, absorption will be the dominant effect. Thus refraction is only of interest when the electron concentration is below this range.

ELECTRON CONCENTRATION

To maintain an electron concentration of 10^9 e/cm^3 by thermal collisions alone requires a local temperature, T , of about 2500° K for

sea level conditions. However the ionization generated by the neutrons and delayed gamma rays from the fission debris can maintain this concentration to a much lower temperature. The gamma source is in general the more significant, although at early times and close-in the neutrons can be of equal significance. Reference 1 gives the gamma ray ionization source as

$$q_Y = \frac{2 \times 10^{19} W_F \rho}{4\pi R^2 (1+t)^{1.2}} e^{-\mu \int \rho dr}, \quad \text{ion pairs cm}^{-3} \text{ sec}^{-1} \quad (\text{I-6})$$

where

W_F = fission yield (MT)

ρ = air density at the field point (gm cm^{-3})

R = range from the source to the field point (km)

t = time after detonation (sec) .

μ = mass absorption coefficient ($\text{cm}^2 \text{ gm}^{-1}$)

In the following we are interested in the shocked region as the shock becomes transparent. This occurs at a shock temperature which is only weakly dependent on yield, thus the shock radius to be used in calculating q scales approximately as the cube root of the yield. The fraction of the total yield which is fission is of course an unknown, but 1/2 is a reasonable nominal value for megaton class yields. This fraction tends to be larger for small yields. The intervening absorption ($e^{-\mu \int \rho dr}$) increases with yield causing a decrease in q as the yield increases. As a result of these various factors, q/ρ in the region of interest will vary less rapidly than the cube root of total yield. Furthermore the prediction of N_e and absorption will be shown to vary as the square root of q . Thus the final conclusion is only weakly dependent on the inputs chosen for Equation 6. To represent a nominal one-megaton surface burst we will choose $W_F = \frac{1}{2}$ MT, $R = 1$ km, $t = .3$ sec and $e^{-\mu \int \rho dr} = \frac{1}{2}$, and obtain

$$q_Y = 3 \times 10^{17} \rho .$$

To approximately account for neutrons we will double this and use

$$q = 6 \times 10^{17} \rho, \quad \text{ion pairs cm}^{-3} \text{ sec}^{-1}. \quad (\text{I-7})$$

The quasi-equilibrium solution of the rate equations for the electron concentration, as given in Reference 1, is*

$$N_e = \sqrt{\frac{q}{\alpha}} \frac{\sqrt{q\alpha} + D}{\sqrt{q\alpha} + D + A}, \quad \text{cm}^{-3} \quad (\text{I-8})$$

where

$$\alpha = \frac{A\alpha_j + D\alpha_d}{A + D}, \quad \text{cm}^3 \text{ sec}^{-1}, \quad (\text{I-9})$$

α_j = ion-ion recombination coefficient

$$= 3 \times 10^{-8} + 6 \times 10^{-6} \frac{P}{T^{2.5}}, \quad \text{cm}^3 \text{ sec}^{-1} \quad (\text{I-10})$$

α_d = electron-ion recombination coefficient

$$= \frac{9 \times 10^{-5}}{T}, \quad \text{cm}^3 \text{ sec}^{-1} \quad (\text{I-11})$$

A = electron attachment rate

$$= 9.7 \times 10^3 \frac{p^2}{T^3} \exp\left(-\frac{600}{T}\right) + 0.9 \frac{p^2}{T^2}, \quad \text{sec}^{-1} \quad (\text{I-12})$$

* In these equations, p is the pressure in dynes per cm² and T is the absolute temperature in degrees Kelvin.

D = electron detachment rate which is the sum of collisional detachment, D_c , resulting from high temperatures and photo detachment D_p caused by energetic photons emitted by the fireball. The collisional detachment coefficient is given in Reference 1 as

$$D_c = 2.4 \times 10^4 \frac{p}{\sqrt{T}} \exp\left(-\frac{5590}{T}\right) + 2.1 p \sqrt{T} \exp\left(-\frac{4990}{T}\right), \text{ sec}^{-1} \quad (\text{I-13})$$

The photo detachment coefficient is given in Reference 2 as

$$D_p = \left(\frac{R_F}{R}\right)^2 1.36 \times 10^{-16} T_F^{5.4}, \text{ sec}^{-1} \quad (\text{I-14})$$

where T_F is the effective radiating temperature ($^{\circ}\text{K}$) and $\left(\frac{R_F}{R}\right)$ is the ratio of the fireball radius to the range to the point of interest (which we shall take to be unity.)

To compute values for the above reaction rates and estimate the relative importance of the various terms we will use ambient conditions corresponding to surface values for the mid United States, i.e., an altitude of about 4000 ft, where the ambient density is about $1.1 \times 10^{-3} \text{ gm/cm}^3$ and the ambient pressure is $9 \times 10^5 \text{ dynes/cm}^2$. Earlier studies have shown that temperatures greater than about 800° K lead to high levels of absorption. We will use a shock temperature of 1000° K and the corresponding values of shock overpressure and density. These are an overpressure ratio, $\Delta p/p$, of 15 and a density compression ratio of 4.4. Then the pressure at the shock front is $1.5 \times 10^7 \text{ dyne/cm}^2$. This yields

$$\begin{aligned} A &= 9.7 \times 10^3 \frac{(1.5 \times 10^7)^2}{(10^3)^3} \exp\left(-\frac{600}{1000}\right) + 0.9 \frac{(1.5 \times 10^7)^2}{(10^3)^2} \\ &= 1.2 \times 10^9 + 2 \times 10^8 = 1.4 \times 10^9, \text{ sec}^{-1} \end{aligned}$$

(Note that the first term dominates for these conditions)

$$\alpha_j = 3 \times 10^{-8} + 6 \times 10^{-6} \frac{1.5 \times 10^7}{(10^3)^{2.5}}$$

$$= 3 \times 10^{-8} + 2.85 \times 10^{-6} = 2.9 \times 10^{-6}, \text{ cm}^3/\text{sec}$$

(Note that the second term dominates)

$$\alpha_d = \frac{9 \times 10^{-5}}{10^3} = 9 \times 10^{-8}, \text{ cm}^3/\text{sec}$$

$$D_c = 2.4 \times 10^4 \frac{(1.5 \times 10^7)}{\sqrt{10^3}} \exp\left(-\frac{5590}{1000}\right) +$$

$$2.1(1.5 \times 10^7) \sqrt{10^3} \exp\left(-\frac{4990}{1000}\right)$$

$$= 4.25 \times 10^7 + 6.8 \times 10^6 = 4.9 \times 10^7, \text{ sec}^{-1}$$

$$D_p \approx 1.36 \times 10^{-16} (10,500)^{5.4} \approx 10^6, \text{ sec}^{-1}$$

The last two equations show photo detachment can be ignored (within the shocked zone).

Substituting the above values into Equation I-8 yields an electron concentration at the above specified shock condition of $N_e = 1.1 \times 10^9 \text{ e/cm}^3$, showing we are in the range of conditions that are of interest.

TEMPERATURE DEPENDENCE OF ABSORPTION

We may obtain the dependence of N_e and thus absorption on local temperature and pressure by noting the dominant terms in these equations.

In equation I-9 for α , $A\alpha_i$ dominates the numerator and A dominates the denominator, i.e.,

$$A\alpha_i = (1.4 \times 10^9) (2.9 \times 10^{-6}) = 4 \times 10^3$$

$$\gg D\alpha_d = (5 \times 10^7) (9 \times 10^{-8}) = 5$$

$$\text{and } A = 1.4 \times 10^9 \gg D = 5 \times 10^7.$$

Thus Equation I-9 can be closely approximated by

$$\alpha \approx \alpha_i \approx 3 \times 10^{-6} \quad (\text{I-10a})$$

We may also simplify Equation (I-8) by noting that

$$\sqrt{q\alpha} = [6 \times 10^{17} (4.4) 1.1 \times 10^{-3} (3 \times 10^{-6})]^{1/2} = 9 \times 10^4 \ll D$$

Thus Equation (I-8) becomes

$$N_e \approx \frac{D}{A} \frac{q}{\alpha_i}, \text{ cm}^{-3} \quad (\text{I-15})$$

Now by using only the dominant terms in D , A , and α_i

$$N_e \approx \frac{2.4 \times 10^4 \frac{\rho}{\sqrt{T}} \exp\left(-\frac{5590}{T}\right)}{9.7 \times 10^3 \frac{\rho^2}{T^3} \exp\left(-\frac{600}{T}\right)} \left[\frac{6 \times 10^{17} \rho}{6 \times 10^{-6} \frac{\rho}{T^{2.5}}} \right]^{1/2}$$

$$= 2.5 \frac{T^{2.5}}{\rho} \exp\left(-\frac{4990}{T}\right) \left[10^{23} \frac{\rho}{\rho} T^{2.5} \right]^{1/2}$$

we may use the gas law to simplify the square-root term i.e.,

$$\frac{p}{\rho} = \frac{R_0}{M} T = 2.9 \times 10^6 T$$

and that term becomes

$$[\quad]^{1/2} = 2 \times 10^8 T^{3/4} .$$

The resulting approximate formula yields predictions that are a few percent higher than those obtain using all terms. To obtain agreement at 1000° K we will use

$$\begin{aligned} N_e &= 4.3 \times 10^8 \frac{T^{3.25}}{p} \exp\left(-\frac{4990}{T}\right) , \quad \text{cm}^{-3} & (I-16) \\ &= 4.3 \times 10^8 \frac{F(T)}{p} \end{aligned}$$

where

$$F(T) = T^{3.25} \exp\left(-\frac{4990}{T}\right) . \quad (I-17)$$

For convenience this function is plotted in Figure I-1.

Equation I-16 may be substituted into the absorption equations to relate absorption directly with temperature, pressure and frequency. From Equation (I-1), (I-2) and (I-16)

$$A_b = \frac{8.5 \times 10^{13} g F(T)}{7.3 \times 10^8 (g p)^2 + (h f)^2} , \quad \text{db/m} \quad (I-18)$$

when $\omega \ll \nu$, then this reduces to

$$A_b = 2 \times 10^5 \frac{F(T)}{p^2} , \quad \omega \ll \nu , \quad \text{db/m} \quad (I-19)$$

and in the other limit of $\omega > \nu$, then

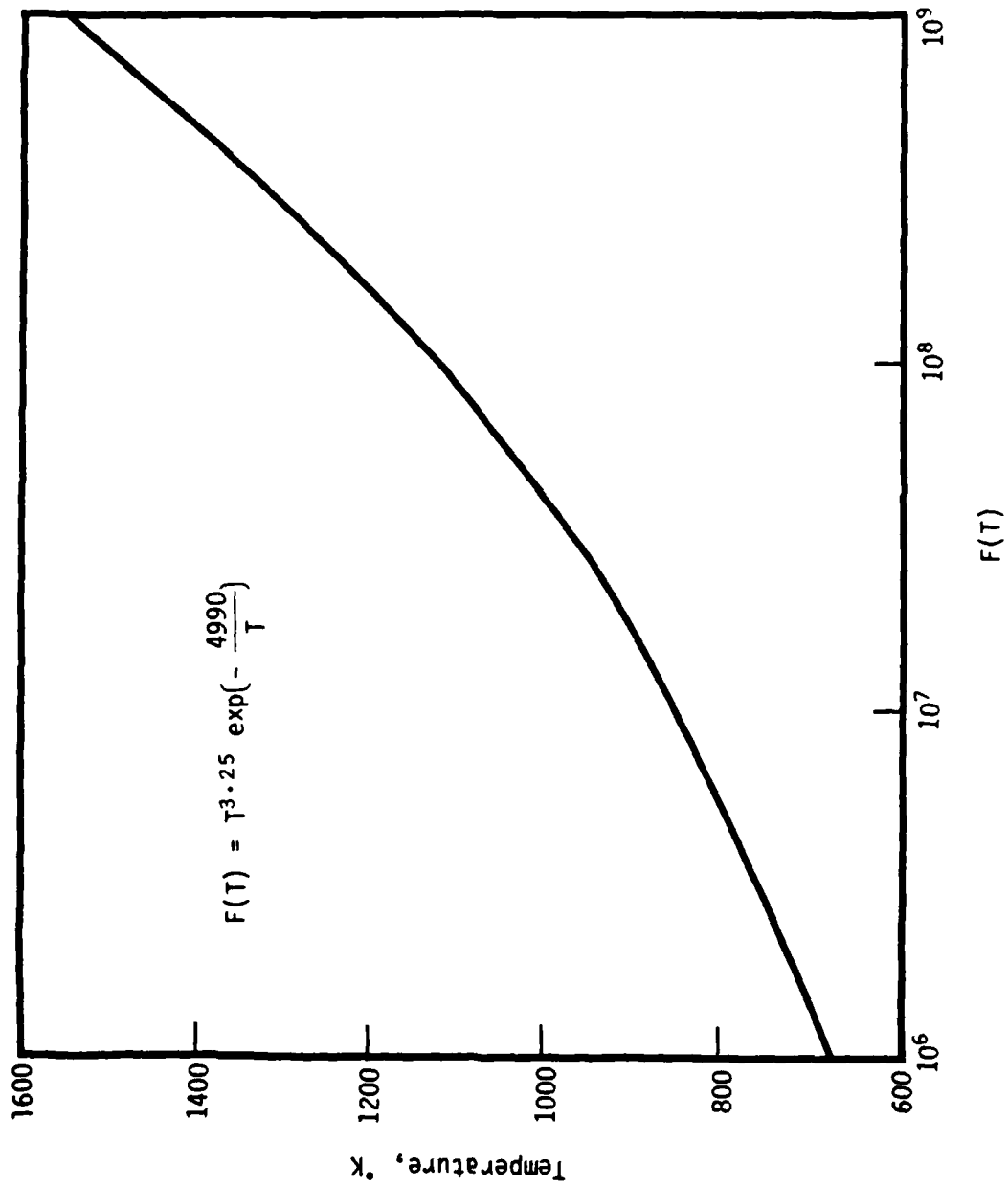
$$A_b = 8.5 \times 10^{13} \frac{F(T)}{f^2}, \quad \omega \ll \nu, \quad \text{db/m} \quad (\text{I-20})$$

MAXIMUM TEMPERATURE FOR REFRACTION

In order to specify the temperatures above which absorption dominates we must make worst case assumptions about the path and the system. The path length will be shortest for a small yield - but even the shock of a 5 kt burst is about 250 meters in radius when it becomes transparent. Perhaps one-tenth of this is a minimum path length. If we also choose 20 db two-way loss as a system limiting factor, then for typical radar frequencies we will use $A_b \approx \frac{1}{2}$ db/m. By inverting Equation 19 and using a shock pressure of about 15 atmospheres we obtain $F(T) = 5 \times 10^8$. Figure I-1 shows this corresponds to a temperature of 1400°K . Note that this high shock pressure also implies an increase in the applicable frequency range of Equation I-19, since ν is proportional to p .

The above temperature is higher than previously suggested as an upper limit primarily because the path length chosen is quite small. When the path length through the shock region is chosen as 100 meters, then this temperature drops to 1130°K . We have also assumed the absorption is uniform along the path in the shock. Since it is not - i.e., it depends on p^{-2} , then the above temperature is an overestimate. For convenience in setting up the refraction calculation we will somewhat arbitrarily use 1200°K as our upper cut off.

There are several assumptions in the above discussion that should not strongly limit the more general applicability of the result. For example, the ranges considered and the fission yield and the doubling to account for the neutrons are all consistent with a nominal 1 MT near-surface burst. Shifting to a nominal small yield would cause several nearly compensating changes in the numbers, but the resulting shock temperature to give specified db levels would change only slightly.



REFERENCES

1. Knapp, W. S. and K. Schwartz. Aids for the Study of Electromagnetic Blackout, DASA 3499H, February 1975.
2. Archer, D. H., Reaction Rate Coefficients for Ambient and Heated Air, DASA 1437, November 1963.

APPENDIX II
SUBROUTINE LISTINGS

```
PROGRAM HLAST
C
C DRIVER FOR TEST OF REFRACTION ERROR
C
C INCLUDE 'GIVEN.C'
C LOGICAL CONTINUE
C OPEN(UNIT=2,NAME='USER1;REFRACT.OUT',STATUS='NEW')
C CONTINUE = .FALSE.
C ICASE = 1
C
C 10 ICASE = ICASE+1
C WRITE(2,1000)ICASE
C 1000 FORMAT(' INPUT FOR CASE NUMBER ',I3)
C
C CALL GETINPUT(CONTINUE)
C CALL REFRACT(DTHETA)
C
C WRITE(2,1050)DTHETA
C 1050 FORMAT(' REFRACTIVE ERROR IS ',1P(13.6))
C
C ANOTHER SET OF INPUT DATA
C IF (CONTINUE) GO TO 10
C
C END OF INPUT DATA
C CLOSE(UNIT=2)
C END
```

```

SUBROUTINE GETINPUT(MOREDATA)
C
C READS INPUT FROM REFRACT.DAT
C TRANSFERS THE DATA VIA THE COMMON BLOCK GIVEN.CMN
C
C LOGICAL EQUAL, MOREDATA
C INCLUDE 'GIVEN.CMN'
C
C DIMENSION IHOL(80), IH(2), IRHOA(5), ITEMPA(6), TWATER(6),
1 IRHS(4), IRTS(4), ITHETA1(7), ICOMMENT(3),
2 IEND(4), ITIME(5)
C
C DATA IH/1,1HW/,
1 IRHOA/4,1HR,1HH,1HD,1HA/,
2 ITEMPA/5,1HT,1HE,1HM,1HP,1HA/,
3 IWATER/5,1HW,1HA,1HT,1HE,1HR/,
4 IRHS/3,1HR,1HH,1HS/,
5 IRTS/3,1HR,1HT,1HS/,
6 ITHETA1/6,1HT,1HH,1HE,1HT,1HA,1H1/,
7 ICOMMENT/2,1HC,1HT/,
8 IEND/3,1HE,1HN,1HD/,
9 ITIME/4,1HT,1HI,1HM,1HE/
C
C DATA RHOA/1,225E-3/, TEMPA/288./, WATER/0.91/
C
C IF (MOREDATA) GO TO 10
C OPEN(UNIT=1,NAME='USER1:REFRACT.DAT',STATUS='OLD',READONLY)
C GET ONE LINE OF INPUT
C
10 READ(1,1MS0,END=600) IHOL
1MS0 FORMAT(80A1)
C
C SKIP THE LINE IF IT IS A COMMENT
C CALL MOLFUL(IHOL,ICOMMENT,EQUAL,.FALSE.,NSKIP)
C IF (EQUAL) GO TO 10
C
C CALL MOLFUL(IHOL,IRHOA,EQUAL,.TRUE.,NSKIP)
C IF (EQUAL) GO TO 11
C
C CALL MOLFUL(IHOL,ITEMPA,EQUAL,.TRUE.,NSKIP)
C IF (EQUAL) GO TO 12
C
C CALL MOLFUL(IHOL,IWATER,EQUAL,.TRUE.,NSKIP)
C IF (EQUAL) GO TO 13

```

```

C      CALL MOLEWL(IMOL,IMMS,EQUAL,,.TRUE.,NSKIP)
      IF (EQUAL) GO TO 174
C      CALL MOLEWL(IMOL,IRTS,EQUAL,,.TRUE.,NSKIP)
      IF (EQUAL) GO TO 184
C      CALL MOLEWL(IMOL,ITHETA,EQUAL,,.TRUE.,NSKIP)
      IF (EQUAL) GO TO 194
C      CALL MOLEWL(IMOL,ITIME,EQUAL,,.TRUE.,NSKIP)
      IF (EQUAL) GO TO 204
C      CALL MOLEWL(IMOL,IM,EQUAL,,.TRUE.,NSKIP)
      IF (EQUAL) GO TO 144
C      END OF DATA SET?
C      CALL MOLEWL(IMOL,IEND,EQUAL,,.FALSE.,NSKIP)
      IF (EQUAL) GO TO 544
C
C      ERROR = UNRECOGNIZABLE INPUT
      WRITE(2,1064)IMOL
1064  FORMAT(' UNRECOGNIZABLE INPUT',5X,A41)
      STOP
C
C      READ W (YIELD)
C
1074  BACKSPACE 1
      READ(1,1074) W
1075  FORMAT(<NSKIP>X,E20.0)
      IF (W.LT.1.E-3) WRITE(2,1075)
1075  FORMAT(' WARNING: INPUT YIELD IS LESS THAN 1 TON')
      IF (W.LE.W.0) THEN
        WRITE(2,1076) W
1076  FORMAT(' ERROR: YIELD =',PF10.4,' IS NEGATIVE OR ZERO. PROGRAM
1 EXITS. ')
        STOP
      ENDIF
      GO TO 14
C
C      READ RHOA (DENSITY)
C
110  BACKSPACE 1
      READ(1,1070)RHOA
      IF (RHOA.LT.1.E-6) WRITE(2,1080)
1080  FORMAT(' WARNING: INPUT DENSITY IS LESS THAN 1E-6.
1RLAST MODEL IS SUSPECT. ')
      GO TO 14

```

```

C
C   READ TEMPA (AMBIENT TEMP.)
C
12W  BACKSPACE 1
    READ(1,1070) TEMPA
    IF (TEMPA.LT.100) THEN
    WRITE(2,1085)
1085 FORMAT(' WARNING: INPUT AMBIENT TEMP IS VERY SMALL OR
1 NEGATIVE. NOMINAL VALUE OF 288K USED. ')
    TEMPA=288.
    ENDIF
    GO TO 10

C
C   READ WATER
C
13W  BACKSPACE 1
    READ(1,1070) WATER
    IF (WATER.LT.0.0) THEN
    WRITE(2,1090)
1090 FORMAT(' WARNING: INPUT VALUE OF WATER VAPOR IS NEGATIVE.
1 DRY AIR IS USED. ')
    WATER=0.0
    ENDIF
    GO TO 10

C
C   READ RRS (RANGE FROM SOURCE TO BURST)
C
17W  BACKSPACE 1
    READ(1,1070) RRS
    IF (RRS.LT.0.0) THEN
    WRITE(2,1092) RRS
1092 FORMAT(' ERROR: RANGE FROM SOURCE TO BURST =',PE10.4,' IS
1 NEGATIVE. PROGRAM EXITS. ')
    STOP
    ENDIF
    GO TO 10

C
C   READ RTS (RANGE FROM SOURCE TO TARGET)
C
18W  BACKSPACE 1
    READ(1,1070) RTS
    IF (RTS.LT.0.0) THEN
    WRITE(2,1095) RTS
1095 FORMAT(' ERROR: RANGE FROM SOURCE TO TARGET =',PE10.4,' IS
1 NEGATIVE. PROGRAM EXITS. ')
    STOP
    ENDIF
    GO TO 10

```

```

C
C   READ THETA1 (ANGLE BETWEEN VECTORS RBS AND RTS)
C
194  BACKSPACE 1
    READ(1,1474) THETA1
    IF (THETA.LT.0.0) THEN
2000  WRITE(2,2000) THETA1
    FORMAT(' ERROR: THETA1 =',PE14.4,' IS NEGATIVE. PROGRAM EXITS.')
```

```

    STOP
    ENDIF
    GO TO 16

C
C   READ TIME
C
204  BACKSPACE 1
    READ(1,1479) TIME
    IF (TIME.LF.0.0) THEN
2045  FORMAT(' ERROR: TIME ',PE14.4,' IS NEGATIVE. PROGRAM EXITS')
```

```

    STOP
    ENDIF
    GO TO 14

C
C   END STATEMENT
C
594  CONTINUE
    MOREDATA = .TRUE.
    GO TO 654

C
C   END OF FILE
C
604  CONTINUE
    MOREDATA = .FALSE.
    CLOSE(UNIT=1)
    GO TO 654

C
C
654  WRITE(2,6065)
9066  FORMAT(' ')
    WRITE(2,6065)
9066  FORMAT('          INPUT DATA ')
    WRITE(2,6071) W
9071  FORMAT(' W (YIELD) .....',1PE13.6)
    WRITE(2,6072) RHOA
9072  FORMAT(' RHOA (DENSITY) .....',1PE13.6)
    WRITE(2,6073) TEMPA
9073  FORMAT(' TEMPA (AMBIENT TEMP.) .....',1PE13.6)
    WRITE(2,6074) WATER
```

```

9074 FORMAT(' WATER .....',1PE13.6)
      WRITE(2,9078) RRS
9078 FORMAT(' RRS (MURST-SOURCE DISTANCE) ....',1PE13.6)
      WRITE(2,9079) RTS
9079 FORMAT(' RTS (TARGET-SOURCE DISTANCE) ...',1PE13.6)
      WRITE(2,9080) THETA1
9080 FORMAT(' THETA1 .....',1PE13.6)
      WRITE(2,9081) TIME
9081 FORMAT(' TIME .....',1PE13.6)
      WRITE(2,9082)

```

C

```

      RETURN
      END

```

C

C

```

      SUBROUTINE MOLENL(IONE,ITWO,ANS,LENGTH,ISKIP)

```

C

C

C

C

C

C

C

```

      LOGICAL LENGTH, ANS
      DIMENSION IONE(1),ITWO(1)
      DATA IHLANK/1H /,IFWU/1H /
      ANS=.FALSE.
      ISKIP=0
      J=0
      N=ITWO(1)+1
      DO 10 I=2,N
2    J=J+1
      IF(IONE(J).EQ.IHLANK) GO TO 2
      IF(IONE(J).NE.ITWO(I)) GO TO 10
10   CONTINUE
      ANS=.TRUE.
      IF(LENGTH) GO TO 15
      RETURN
15   CONTINUE
      K=J
      DO 20 L=K,AN
      J=J+1
      IF(IONE(J).EQ.IFWU) GO TO 30
20   CONTINUE
30   ISKIP=J
100  RETURN
      END

```

```

SUBROUTINE REFRACT(DTHETA)
C
  INCLUDE 'GIVEN.CMN'
  INCLUDE 'WERT.CMN'
  DATA RH07/1.225E-3/,TEMPZ/288./
  HALFPI=ASIN(1./4)
  PI=2*HALFPI
C
  DTHETA=.0
  W3=(W+RH0Z/RH0A*TEMPZ/TEMPA)**(1./3.)
  STIME=TIME/W3
  CALL DENSITY(STIME)
C
  TEST FOR IONIZATION
  IF (TEMPK.LE.1200.) GO TO 1W
  WRITE(2,RH07)
  8W00 FORMAT(' SHOCK STRONG ENOUGH TO CAUSE ABSORPTION, REFRACTION
  I IGNORED')
  GO TO 8W0
C
  R1 IS THE RANGE FROM SOURCE TO POINT OF CLOSEST APPROACH
  1W R1=RHS*COS(THETA1)
  SRAD=PRAD+W3
  RTR=SQRT(RHS**2+RTS**2-2*RHS*RTS*COS(THETA1))
  RMIN=RHS*SIN(THETA1)
  LASTIME=0
C
  IF SHOCK HAS NOT REACHED LINE OF SIGHT, DO NOTHING.
  IF (RMIN.GE.SRAD) GO TO 4W
C
  IF SHOCK HAS NOT CROSSED LINE OF SIGHT, DO NOTHING.
  IF ((RTR.GE.SRAD).AND.(RTS.LT.R1)) GO TO 4W
  IF ((RHS.GE.SRAD).AND.(R1.LT.0)) GO TO 4W
  GO TO 5W
  4W CONTINUE
  WRITE(2,RH17)
  8W10 FORMAT(' SHOCK HAS NOT REACHED LINE OF SIGHT.')
  GO TO 8W0
C
  5W CONTINUE
  SIPSIN=(RMIN/SRAD)
  PSIN=ASIN(SIPSIN)
  ETAS=1.+0.22*RH0A*(1.+4.*RE+3*WATER/TEMPA)
C
  DEFINE ETAS,CUNMAX,AND CONST
  STRT=AMINI(SRAD,AMAXI(RHS,RTR))
  STRTS=STRT/W3
  CALL ETA(STRTS,RH01,TEMP1,ETAS)
  SML=AMINI(SRAD,AMINI(RHS,RTR))
  SMLS=SML/W3

```

```

CALL ETA(SMLS,RHO1,TEMP1,ETAM)
CONMAX=SMLS*ETAM
IF (SRT.EQ.SRAD) THEN
  CONST=PRAD*ETA,*SIPSI*
ELSE
  IF (SML.EQ.RHS) THEN
    CONST=CONMAX*SIN(THETA1)
  ELSE
    SRHS=RHS/W3
    CALL ETA(SRHS,RHO1,TEMP1,ETA,SRHS)
    CONST=SRHS*ETA,SRHS*SIN(THETA1)
  ENDIF
ENDIF

```

```

64 LOOPC=0

```

C
C
C
C
C
C

```

IF (SRAD.GT.AMIN(RHS,RTH)) GO TO 94

```

```

      COMPLETE TRAVERSAL - BOTH TARGET AND SOURCE ARE OUTSIDE SHOCK
      INTEGRATE FROM SRAD TO RMIN

```

```

      RECALC RMIN USING ETA AT RMIN

```

```

SRMIN=RMIN/W3
CALL ETA(SRMIN,RHO1,TEMP1,ETARMIN)
RMIN=RMIN+ETARMIN/ETA1

```

```

75 DUM1=PRAD

```

```

DUM2=RMIN/W3

```

```

ETANEW=ETA1

```

```

CALL INTEGRT(DUM1,DUM2,CONST,ETANEW,PHI,-1)

```

```

ETARMIN=ETANEW

```

```

ETABAR=CONST/PRAD/COS(PHI)

```

```

DTHETA=(SRAD+SQRT(ETABAR)-RMIN)/(RHS+COS(THETA1))

```

```

IF (LASTIME.EQ.1) GO TO 84

```

```

SIPSI=RHS/SRAD*SIN(THETA1+DTHETA)

```

```

PSI=ASIN(SIPSI)

```

C

```

LOOPC=LOOPC+1

```

```

CONST=CONST

```

```

CONST=ETA1*PRAD*SIPSI

```

```

RMIN=CONST*W3/ETARMIN

```

```

IF (CONST.GE.CONMAX) THEN

```

```

  CONST=CONMAX

```

```

  RMIN=CONST*W3/ETARMIN

```

```

  LASTIME=1

```

```

  ENDIF

```

```

GO TO 75

```

```

C
C      INTEGRATE ALL CASES WHERE
C      TARGET OR SOURCE OR BOTH ARE INSIDE SHOCK
C 94 THETA3=ASIN(RTS/RTS+SIN(THETA1))
C      ASIN RETURNS VALUES BETWEEN -HALFPI AND HALFPI
C      CHECK IF THETA3 SHOULD BE GREATER THAN HALFPI
C      IF ((R1.LE.0).OR.(RTS.LE.R1)) GO TO 95
C      THETA2=ASIN(RHS/RTS+SIN(THETA1))
C      IF ((THETA1+THETA2).LT.HALFPI) THETA3=PI-THETA3
C
C 95 CONTINUE
140 DUM1=AMIN1(RHS,SRAD)/W3
C      DUM2=AMIN1(RTH,SRAD)/W3
C      ETANW=ETAS
C      DPHIDK=1.
C      CALL INTEGRT(DUM1,DUM2,CONST,ETANW,PHI,DPHIDK)
C
C      IF ((R1.LE.0).OR.(RTS.LE.R1)) GO TO 150
C
C      LINE OF SIGHT CROSSES POINT OF CLOSEST APPROACH
C      ADDITIONAL INTEGRATION
C      DUM1=AMIN1(RHS,RTH)/W3
C      DUM2=RMIN/W3
C      DPHIDK=1.
C      CALL INTEGRT(DUM1,DUM2,CONST,ETANW,PHI,DPHIDK)
C      PHI=PHI+2*DPHIDK
C      DPHIDK=DPHIDK+2*DPHIDK
C      ETARMIN=ETANW
C
C
C 150 IF (RHS.LT.SRAD) GO TO 175
C      SOURCE IS OUTSIDE AND TARGET IS INSIDE SHOCK
C      L=SQRT(RHS**2+SRAD**2-2*RHS*SRAD*COS(THETA3-PHI))
C      DTHETA=ASIN(SRAD/L+SIN(THETA3-PHI))-THETA1
C      IF (LASTIME.EQ.1) GO TO 160
C      PSIN=THETA3-PHI+THETA1+DTHETA
C
C      ITERATION LOOP
C      LOOPC=LOOPC+1
C      CONST=CONST
C      CONST=PRAD*ETA4+SIN(PI/4)
C      RMIN=CONST*W3/ETARMIN
C      IF (CONST.GE.CONMAX) THEN
C          CONST=CONMAX
C          RMIN=CONST*W3/ETARMIN
C          LASTIME=1
C          ENDOF
C      GO TO 140

```

```

C
C
175 IF (RTR.LT.SPAD) GO TO 200
C      SOURCE IS INSIDE AND TARGET IS OUTSIDE SHOCK
C      C=SQRT(RTR**2+SRAD**2-2*RTR*SRAD*COS(THETA3-PHI))
C      PSIN=ASIN(RTR/C*SIN(THETA3-PHI))-HALFPI
C      IF (LASTIME.EQ.1) GO TO 180
C
C      ITERATION LOOP
C      LOOPC=LOOPC+1
C      CONST=CONST
C      CONST=PNAD*ETA* SIN(PSI)
C      RMIN=CONST*W3/ETARMIN
C      IF (CONST.GE.CONMAX) THEN
C          CONST=CONMAX
C          RMIN=CONST*W3/ETARMIN
C          LASTIME=1
C          ENDIF
C      GO TO 100
C
C 180 SRHS=RHS/W3
C      CALL ETA(SRHS,RHU1,TEMP1,ETARHS)
C      DTHETA=ASIN((SRAD*ETA* SIN(PSI))/(RHS+ETARHS))-THETA1
C      GO TO 100
C
C
C      SOURCE AND TARGET ARE INSIDE SHOCK
C 200 IF (LASTIME.EQ.1) GO TO 250
C
C      ITERATION LOOP
C      LOOPC=LOOPC+1
C      CONST=CONST
C      CONST=(THETA3-PHI)/DHU1+CONST
C      RMIN=CONST*W3/ETARMIN
C      IF (CONST.GE.CONMAX) THEN
C          CONST=CONMAX
C          RMIN=CONST*W3/ETARMIN
C          LASTIME=1
C          ENDIF
C      GO TO 100
C
C
C 250 SRHS=RHS/W3
C      CALL ETA(SRHS,RHU1,TEMP1,ETARHS)
C      DTHETA=ASIN(CONST/(RHS+ETARHS))-THETA1
C
C 800 RETURN
C      END

```

```

SUBROUTINE INTEGRT(RS, RM, CK, ETANEW, PHI, DPDK)
C
C INPUT
C   RS = LIMIT OF INTEGRATION
C   RM = LIMIT OF INTEGRATION
C   CK = CONSTANT
C   ETANEW = INDEX OF REFRACTION AT THE UPPER LIMIT OF INTEGRATION
C OUTPUT
C   PHI = ANGLE BETWEEN THE VECTORS RS AND RM
C   DPDK = THE DERIVATIVE OF PHI WITH RESPECT TO THE CONSTANT
C
C   INCLUDE 'WFRT.CMN'
C   INCLUDE 'GIVEN.CMN'
C   DATA NUM/50/, TESTL/0.01/, TESTS/0.002/
C
C   ETA0=ETANEW
C   R1=AMAX1(RS, RM)
C   R2=AMIN1(RS, RM)
C   I=0
C   SUM1=0
C   SUM2=0
C   IF (ETA0.NE.ETAC)
C     STEP=(R1-R2)/FLIAT(NUM)
C     RAD1=R1
10  RAD2=AMAX1(R2, RAD1-STEP)
C     IF (RAD2.LE.R2) STEP=RAD1-RAD2
C     RADC=(RAD2+RAD1)/2.
C     I=I+1
C     IF (I.GT.NUM*2) GO TO 20
C     CALL ETA(RADC, X1, X2, ETAC)
C
C     TEST=ABS(ETA0-ETAC)/(ETA0+1.)
C     IF (TEST.LE.TESTL) GO TO 20
C
C     STEP=STEP/2.
C     GO TO 10
C
C 20  C1=CK/ETAC/RAD1
C     C2=AMIN1(1., CK/ETAC/AMAX1(R2, RAD2))
C     D1=ACOS(C1)-ACOS(C2)
C     SUM1=SUM1+D1
C     IF (AMAX1(C1, C2).GE.1.) GO TO 30
C     IF (DPDK.LT.0.) GO TO 25
C     D2=1./SQRT(1./C1**2-1.)-1./SQRT(1./C2**2-1.)
C     SUM2=SUM2+D2
C
C 25  IF (RAD2.LE.R2) GO TO 30
C     ETAN=ETAC
C     RAD1=RAD2

```

```
C      IF (TEST.LF.TESTS) STEP=STEP+2.  
      IF (C2.LT.1.0) GO TO 10  
30    PHI=SUM1  
      DPLK=SUM2/CK  
      FTANE=ETAC  
      RETURN
```

```
C      200 CONTINUE  
      WRITE(2,1014)  
1010 FORMAT(' ERROR: INTEGRATION ROUTINE HAS EXCEEDED THE MAXIMUM  
      1 NUMBER OF LOOPS. PROGRAM EXITS.')
```

```
      STOP  
      END
```

```

SUBROUTINE ETA(SH,RHOR,TEMPR,ETAR)
C
C   INPUT
C   SH = SCALED RANGE (CM)
C   OUTPUT
C   RHOR = DENSITY (DYNE/CM2)
C   TEMPR = TEMPERATURE (DEGREES K)
C   ETAR = INDEX OF REFRACTION
C
C   CALCULATES RHOR AND TEMPR FROM 1 KI STANDARD, AND
C   THEN ETAR AT SCALED RANGE
C
INCLUDE 'GIVEN.CMN'
INCLUDE 'DENSITY.CMN'
DATA RHOZ/1.225E-3/
CALL DENS(SH)
RHOR=RHOA*(1.+ODR/RHOZ)
TEMPR=AMAX1(TEMPA,TEMPK*((1.+ODR)/(1.+ODPK))+N.4)
ETAR=1.+N.22*RHOA*(1.+4.8E3*WATER/TEMPR)
RETURN
END

```

```

SUBROUTINE AIRPT (EEF,RRR,GMONE,PRES,TEMP)
C
C DOAN-NICKLE EQUATION OF STATE OF AIR (SEMI-PHYSICAL FIT)
C AS EXTRACTED FROM MDAC FEB 82 VERSION OF LAMB
C
C INPUT
C EEE = ENERGY (ERGS/GM)
C RRR = DENSITY (GM/CM3)
C OUTPUT
C GMONE = GAMMA = 1
C PRES = PHESSURE (DYNE/CM2)
C TEMP = TEMPERATURE (DEGREES K)
C
C
C IGO=1
C GO TO 1
C
C THIS ENTRY RETURNS ONLY GMONE
C ENTRY AIR(EEF,RRR,GMONE)
C IGO=0
C
C 1 E=EEE*1.F=10
C RHO=RRR/1.293E-3
C E1=(8.5-F)/.975
C IF (ABS(F1).LT.5.4) GO TO 3
C
C IF (E1.GT.0.0) GO TO 2
C
C F0=0.0
C FON=EXP(-E/6.63)
C WS=0.0
C GO TO 4
C
C 2 F0=EXP(-E/4.46)
C FON=0.0
C WS=1.0
C GO TO 4
C
C 3 DF1=.975*(RHO)**.45
C FE1=8.5+0.155*42*ALOG(RHO)
C F1=(E1-F)/DF1
C WS=1./(EXP(-F1)+1.)
C F0=EXP(-E/4.46)*WS
C FON=EXP(-E/6.63)*(1.-WS)
C
C 4 RETA=0.0
C IF (E.LE.1.4) GO TO 5

```

```

C      HETA=(6.9487E-03*WS+1.38974E-02)*ALOG(E)
      F2=(E-40.0)/3.0
      IF (ABS(E2).LT.5.0) GO TO 7
C
      IF (E2.GT.0.0) GO TO 6
C
5     FN=0.0
      WS=0.0
      GO TO 8
C
6     FN=EXP(-F/25.5)
      WS=1.0
      GO TO 8
C
7     DF2=4.0*RHO**0.85
      FE2=45.0*RHO**0.157
      F2=(E-FE2)/DF2
      WS=1.0/(EXP(-E2)+1.0)
      FN=EXP(-F/25.5)*WS
C
8     E3=(E-160.0)/6.0
      HETA=BETA*(1.-WS)+.045*WS
      FE=0.0
      IF (E3.GT.(-5.0)) FE=1.0/(EXP(-E3)+1.0)
      GMONE=(.161+.255*FO+.28*FON+.137*FN+.05*FE)*RHO**BETA
C
      IF (IGU.EQ.0) GO TO 10
C
      PRES=GMONE*EFE*PRR
C
C              TEMPERATURE
C
      RHOLN=ALOG(RHO)
      F=(6.582549E-05+RHOLN-2.71434E-03)*RHOLN+9.72E-01
      G=(-2.338785E-05+RHOLN-6.418673E-04)*RHOLN+2.645E-02
      H=(3.923123E-07+RHOLN+5.971549E-06)*RHOLN-9.21E-05
      CON1=3480.0*GMONE*E
      CON2=(H+E*G)*E*F
      BETA=(E-3.0)/0.66
C
      IF (HETA.GT.19.0) GO TO 9
C
      TEMP=CON1/(CON2*(1.4-CON2)/(EXP(HETA)+1.0))
      GO TO 10
C
9     TEMP=CON1/CON2
C
10    RETURN
      END

```

SUBROUTINE DENSITY (T)

PROVIDES BLAST PARAMETERS AT INPUT TIME "T" BASED ON
NUCLEAR BLAST STANDARD - 1 KT, AFNL-TR-73-55, REV APRIL 1975

INITIAL CONDITIONS ASSUMED TO BE STP, I.E.
AMBIENT PRESSURE = 1.0125E6 DYNE/CM2
AMBIENT DENSITY = 1.225E-3 GM/CM3

OUTPUT VIA COMMON BLOCK ON INITIAL CALL AT TIME T
PRAD = SHOCK FRONT RADIUS (CM)
OPPK = SHOCK FRONT OVER-PRESSURE (DYNE/CM2)
ODPK = SHOCK FRONT OVER-DENSITY (GM/CM3)
TEMPK = SHOCK FRONT TEMPERATURE (K) -FROM EQUATION OF STATE
OUTPUT ON SUBSEQUENT CALLS AT SAME TIME VIA ENTRY DENS
ODR = OVER-DENSITY AT RADIUS R (GM/CM3)

INCLUDE 'WERT.CMN'

DATA TA3/-26.25/,TPWR1/W.371/,TPWR2/W.79/,
1 AC/3.18E18/,AD/1.00E14/,ASTAR/9.0F9/,HSTAR/4.454E4/,
2 RHOZ/1.225E-3/,
3 H/W.03291/,C/-1.006/,CZ/33897.0/,HZ/8490.0/,
4 BR/W.03499/,CC/-1.068/,
5 TTOLD/2.0/

IF (T.EH.TTOLD) GO TO 9

DETERMINE WFR2 (RADIUS)

1 IF (T.LE.W.3) GO TO 1A
CALCULATE RADIUS EXPLICITLY.
EARLY TIME FORM.

DETERMINE WZP
 $WZP = (1.0 - H * T + C) * (CZ + T * HZ)$

IF (T.LT.W.2H) WFR2=24210.*T**TPWR1*(1.+(1.23*T**0.123)*
1(1.0-EXP(TA3*T**TPWR2)))

IF (T.GT.W.1) GO TO 2
LATE TIME FORM.

ALT=ALOG(T)
ALFT=ALT*3.391R2
RNEW=WZP*1.045E4+2.15E3*ALT+(9.E3/ALFT-6.8E3)/ALFT
INTERMEDIATE TIME INTERPOLATION.

IF (T.(T.W.2H) RNEW=(RNEW*(T-W.1)+WFR2*(W.2R-T))/W.1B
WFR2=RNEW
2 WFR2
PRAD=R

```

C
C   DETERMINE OPPK
C
3  RR=1.0/R
   RTIO=2.24517E-5*R
   CF=SQRT(ALOG(RTIO+3.0*EXP(-(SQRT(RTIO)/3.0))))
   OPPK=((AC*RR+AN)*RR+ASTAR/CF)*RR
C
C   DETERMINE ODPK
C
4  OP=OPPK
   RTIU=OP/1.0125E6
   P=OP+1.0125E6
   GMONE=0.4
   GAMMA=1.4
   GAMKA=GAMMA
C
   DO 5 N=1,20
   RHO1=RHOZ*((2.0+GAMKA+(GAMKA+1.0)*RTIU)/(2.0+GAMKA+(GAMKA-1.0)*RTIU))
   EE=P/(GMONE+RHO1)
   CALL ATRPT (EE,RHO1,GMONE,PHES,TEMPK)
   GAMKAO=GAMKA
   GAMRA=2.0*GMONE/(2.5*GMONE+1.0)+1.0
   IF (ABS(GAMRA-GAMKAO),LT,1.0E-5) GO TO 6
5  CONTINUE
6  ODPK=RHO1-RHOZ
C
C   DETERMINE RZD
C
8  RZD=0.0
   IF (T,LT,0.265) RZD=2.5*ML4*T+0.395
   IF (T,GE,0.265) RZD=(1.0-RR*T+CC)*(CZ+T+HZ)+5MV.0
   RETURN
C
   ENTRY DENS(KAD)
   R=RAD
C
C   DETERMINE ODR
C
9  RPK=PKAD
   IF (T,LT,0.2) GO TO 11
C
   RPK=RPK+1.0E-5
   R=R+1.0E-5
   IF (T,EN,TTOLD) GO TO 10

```

C

```
RZ=HZU
RMN=HZ-9.7163E-3+T**2.12115
RZ=HZ+1.E-5
RMN=RMN+1.E-5
ODMN=-0.5+ODPK+2.2E-5+T**(-1.5020)
RNEG=HZ-RMN
RPLS=RPK-RZ
RNP=RPK-RMN
ALN=ODPK/RPLS
HLN=ODPK-ALN*RPK
ODMNLN=ALN+RMN+HLN
FMLT=ABS(ODMN/ODPK)
ODMHY=ODMN+FMLT*(ODMNLN-ODMN)
ALPHA=(RNP/(ODMHY-ODPK)+RPLS/ODPK)/RNEG
BETA=-RPLS*(ALPHA+1.0/ODPK)
FNGZ=RNP/RPLS
DNOM=ALPHA+RNP+BETA
RCRMN=1.-ODMN/(RNP/ODMN+ODPK)
CRMNLH=ALOG(RCRMN)
CGZL=(BETA+(1.0/RCRMN-1.0)/DNOM)/(FNGZ+CRMNLH+RNP**2*(FNGZ-1.0)**2)
  (RNP+ODPK+DNOM)
RGZ=EXP(CGZL)
HGZL=CRMNLH/CGZL**2*(RNP**2+FNGZ)
RGZ=EXP(HGZL)
```

C

```
10 RHR=RPK-R
GR=1.-RGZL**2*(CGZL**2*(RHR**2+FNGZ))
IF (R.GT.0.7) GR=(RPK-R)/RPLS+GR+(R-RZ)/RPLS
HR=RHK/(ALPHA+RHR+BETA)+ODPK
ODR=GR+HR
RPK=RPK+1.E5
R=R+1.E5
IF (T.GT.1.0) GO TO 13
```

C

```
11 IF (T.EQ.TTOLD) GO TO 12
```

C

```
A=1.2E-3
C=ALOG(-A/(ODPK-A))/(RZ-RPK)
R=(ODPK-A)*EXP(-C*RPK)
```

C

```
12 WFLT=A+H*EXP(C*R)
IF (T.LE.0.2) ODR=WFLT
IF (T.GT.0.2) ODR=(WFLT*(1.-T)+ODR*(T-0.2))*1.25
```

C

```
13 TTOLD=T
RETURN
```

C

```
14 WRITE(2,1000)
1000 FORMAT(' ERROR: TIME MUST BE GREATER THAN ZERO')
STOP
END
```

DISTRIBUTION LIST

DEPARTMENT OF DEFENSE

Assistant to the Secy of Defense
Atomic Energy
ATTN: Executive Asst

Command & Control Tech Ctr
ATTN: C-312, R. Mason
ATTN: C-650

Defense Advanced Rsch Proj Agency
ATTN: STO, S. Zakanycz

Defense Communications Agency
ATTN: Code 205
ATTN: Code 230
ATTN: J300 for Yen-Sun Fu

Defense Communications Engrg Ctr
ATTN: Code R123
ATTN: Code R410, R. Craighill
ATTN: Code R410, N. Jones
ATTN: Code R410

Defense Nuclear Agency
ATTN: RAAE
ATTN: STNA
ATTN: RAAE, P. Lunn
3 cy ATTN: RAAE
4 cy ATTN: TITL

Defense Tech Info Ctr
12 cy ATTN: DD

Dep Under Secy of Defense
Comm, Cmd, Cont & Intell
ATTN: Dir of Intell Sys

Field Command
DNA Det 1
Lawrence Livermore Lab
ATTN: FC-1

Field Command
Defense Nuclear Agency
ATTN: FCPR
ATTN: FCTT, W. Summa
ATTN: FCTXE
ATTN: FCTT, G. Ganong

Interservice Nuclear Weapons School
ATTN: TTV

Joint Chiefs of Staff
ATTN: C3S Evaluation Office, HDOO

Joint Strat Tgt Planning Staff
ATTN: JLTW-2

Under Secy of Def for Rsch & Engrg
ATTN: Defensive Systems
ATTN: Strat & Thtr Nuc Forces, B. Stephan
ATTN: Strat & Space Sys, OS

WMMCCS System Engrg Org
ATTN: R. Crawford

DEPARTMENT OF THE ARMY

US Army Electronics R&D Command
ATTN: DELAS-AS, H. Holt
ATTN: DELAS-EO, F. Niles

BMD Advanced Technology Ctr
ATTN: ATC-R, D. Russ
ATTN: ATC-R, W. Dickinson
ATTN: ATC-T, M. Capps
ATTN: ATC-O, W. Davies

BMD Systems Command
ATTN: BMDSC-HLE, R. Webb
ATTN: BMDSC-LEE, R. Bradshaw
ATTN: BMDATC-R, W. Dickerson
2 cy ATTN: BMDSC-HW

Harry Diamond Labs
ATTN: DELHD-TA-L
2 cy ATTN: DELHD-NW-P

US Army Chem School
ATTN: ATZN-CM-CS

US Army Comm-Elec Engrg InstaI Agency
ATTN: CC-EMEO-PED, G. Lane

US Army Foreign Science & Tech Ctr
ATTN: DRXST-SD

US Army Materiel Dev & Readiness Cmd
ATTN: DRCLDC, J. Bender

US Army Nuc & Chem Agency
ATTN: Library

US Army Satellite Comm Agency
ATTN: Doc Control

US Army TRADOC Sys Analysis Actvty
ATTN: ATAA-PL

US Army White Sands Missile Range
ATTN: STEWS-TN-N, K. Cummings

USA Missile Command
ATTN: DRSMI-RH
ATTN: Documents Section
ATTN: DRSMI-YSO, J. Gamble
2 cy ATTN: Redstone Scientific Info Ctr

DEPARTMENT OF THE NAVY

Naval Electronic Sys Command
ATTN: PME 117-20
ATTN: Code 501A
ATTN: PME 117-2013, G. Burnhart
ATTN: PME 106-4, S. Kearney
ATTN: PME 117-211, B. Kruger
ATTN: PME 106-13, T. Griffin

Naval Intell Support Ctr
ATTN: NISC-50
ATTN: Document Control

DEPARTMENT OF THE NAVY (Continued)

Naval Ocean Systems Ctr
ATTN: Code 532
ATTN: Code 5322, M. Paulson
ATTN: Code 5323, J. Ferguson

Naval Postgraduate School
ATTN: Code 1424, Library

Naval Research Lab
ATTN: Code 7950, J. Goodman
ATTN: Code 2627
ATTN: Code 4700, W. A11
ATTN: Code 4187
ATTN: Code 4701
ATTN: Code 7500, B. Wald
ATTN: Code 4700
ATTN: Code 4780, P. Palmadesso
ATTN: Code 5300
ATTN: Code 6730, E. McClean
ATTN: Code 6700
ATTN: Code 6700, T. Coffey
ATTN: Code 4720, J. Davis
ATTN: Code 2000, J. Brown
ATTN: Code 4780, S. Ossakow

Naval Surface Weapons Ctr
ATTN: Code F31
ATTN: Code X211

Ofc of the Deputy Chief of Naval Ops
ATTN: NOP 941D

Strategic Systems Project Office
ATTN: NSP-43
ATTN: NSP-2722, F. Wimberly
ATTN: NSSP-2722, M. Meserole
ATTN: NSP-2141

Theater Nuclear Warfare Project Ofc
ATTN: PM-23, D. Smith

DEPARTMENT OF THE AIR FORCE

Air Force Geophysics Lab
ATTN: R. O'Neil
ATTN: OPR-1
ATTN: SULL
ATTN: PHY, J. Buchau
ATTN: LKB, K. Champion
ATTN: CA, A. Stair
ATTN: OPR, H. Gardiner
ATTN: R. Babcock

Air Force Tech Applications Ctr
ATTN: Tech Library
ATTN: TFR, C. Meneely
ATTN: TN

Air Force Weapons Lab
ATTN: CA
ATTN: NTYC
ATTN: SUL

Air Force Wright Aeronautical Lab
ATTN: W. Hunt
ATTN: A. Johnson

Air University Library
ATTN: AUL-LSE

DEPARTMENT OF THE AIR FORCE (Continued)

Assistant Chief of Staff
Studies & Analyses
ATTN: AF/SASC, C. Rightmeyer

Ballistic Missile Office
ATTN: PM
ATTN: ENSN, W. Wilson
ATTN: ENBF
ATTN: ENSN
ATTN: ENBE
ATTN: SYC, Col Kwan
ATTN: HQ, Space Div/RSP

Deputy Chief of Staff
Research, Dev, & Acq
ATTN: AFRDS, Space Sys & C3 Dir

Foreign Technology Div
ATTN: NIIS Library

Rome Air Development Center
ATTN: OCS, V. Coyne
ATTN: OCD, J. Simons
ATTN: TSLD

Space Command
ATTN: DC, T. Long

Space Division
ATTN: YGJB, W. Mercer
ATTN: YGJB, P. Kelly
ATTN: YGJ

Space Division
ATTN: YKM, Cpt Norton
ATTN: YKM

Strategic Air Command
ATTN: XPFS, Maj Skluzacek
ATTN: XPFS
ATTN: NRT
ATTN: ADWAT, R. Wittler

DEPARTMENT OF ENERGY

Department of Energy
ATTN: OMA, DP-22

Department of Energy
ATTN: DP-233

OTHER GOVERNMENT AGENCIES

Central Intelligence Agency
ATTN: OSWR/NED
ATTN: OSWR/SSD for K. Feuerpfel

Department of Commerce
ATTN: D. Williams
ATTN: F. Fehsenfeld

Institute for Telecomm Sciences
ATTN: W. Utlaut
ATTN: G. Falcon

Office of International Security Policy
Bureau of Politico Military Affairs
ATTN: PM/STM

NATO

NATO School, SHAPE
ATTN: US Doc Officer

DEPARTMENT OF ENERGY CONTRACTORS

EG&G, Inc
Attention Document Control
ATTN: J. Colvin
ATTN: D. Wright

University of California
Lawrence Livermore National Lab
ATTN: Tech Info Dept Library
ATTN: L-97, T. Donich
ATTN: L-31, R. Hager
ATTN: L-389, R. Ott

Los Alamos National Lab
ATTN: T. Kunkle, ESS-5
ATTN: J. Wolcott
ATTN: MS 664, J. Zinn
ATTN: MS 670, J. Malik
ATTN: R. Jeffries
ATTN: D. Simons
ATTN: MS 670, J. Hopkins

Sandia National Labs
ATTN: D. Thronbrough
ATTN: Org 4231, T. Wright
ATTN: Tech Lib 3141
ATTN: C. Williams
ATTN: Org 7112, C. Mehl
ATTN: D. Dahlgren
ATTN: Org 1250, W. Brown

DEPARTMENT OF DEFENSE CONTRACTORS

Aeroject Electro-Systems Co
ATTN: J. Graham

Aerospace Corp
ATTN: I. Garfunkel
ATTN: G. Anderson
ATTN: D. Olsen
ATTN: J. Reinheimer
ATTN: J. Straus
ATTN: A. Morse
ATTN: V. Josephson, MS-4-933
ATTN: R. Slaughter
ATTN: N. Cohen

Analytical Systems Engrg Corp
ATTN: Radio Sciences

Berkely Research Associates, Inc
ATTN: S. Brecht
ATTN: J. Workman
ATTN: C. Prettie

Boeing Aerospace Co.
ATTN: MS/87-63, D. Clauson

University of California at San Diego
ATTN: H. Booker

Charles Stark Draper Lab, Inc
ATTN: A. Tetewski
ATTN: D. Cox
ATTN: J. Gilmore

DEPARTMENT OF DEFENSE CONTRACTORS (Continued)

Comsat Labs
ATTN: D. Fang

Cornell University
ATTN: M. Kelly
ATTN: D. Farley Jr

E-Systems, Inc
ATTN: R. Berezdivin

Electospace Systems, Inc
ATTN: P. Phillips
ATTN: H. Logston

EOS Technologies, Inc
ATTN: B. Gabbard

ESL, Inc
ATTN: J. Marshall

General Electric Co
ATTN: R. Edsall

General Electric Co
ATTN: G. Millman

General Research Corp
ATTN: B. Bennett

Geo Centers, Inc
ATTN: E. Marram

GTE Communications Products Corp
ATTN: R. Steinhoff

GTE Communications Products Corp
ATTN: J. Concordia
ATTN: I. Kohlberg

Harris Corp
ATTN: E. Knick

Honeywell, Inc
ATTN: A. Kearns MS924-3
ATTN: G. Terry, Avionics Dept

Horizons Technology, Inc
ATTN: R. Kruger

HSS, Inc
ATTN: D. Hansen

Information Science, Inc
ATTN: W. Dudziak

Institute for Defense Analyses
ATTN: E. Bauer
ATTN: H. Gates

International Tel & Telegraph Corp
ATTN: Tech Library

Jamieson Science & Engrg
ATTN: J. Jamieson

Kaman Sciences Corp
ATTN: P. Tracy
ATTN: D. Perio
ATTN: J. Jordano

DEPARTMENT OF DEFENSE CONTRACTORS (Continued)

JAYCOR
ATTN: J. Sperling

Johns Hopkins University
ATTN: K. Potocki

Kaman Tempo
ATTN: W. McNamara
ATTN: K. Schwartz
ATTN: J. Devore
ATTN: DASIAC
ATTN: B. Gambill
ATTN: J. Devore

Kaman Tempo
ATTN: DASIAC

Lockheed Missiles & Space Co, Inc
ATTN: M. Walt
ATTN: R. Johnson
ATTN: J. Kumer
ATTN: R. Sears
ATTN: J. Perez

Lockheed Missiles & Space Co, Inc
2 cy ATTN: D. Churchill

M.I.T. Lincoln Lab
ATTN: D. Towle
ATTN: J. Evans

MA/COM Linkabit Inc
ATTN: A. Viterbi
ATTN: I. Jacobs
ATTN: H. Van Trees

Magnavox Govt & Indus Electronics Co
ATTN: G. White

McDonnell Douglas Corp
ATTN: W. Olson
ATTN: Technical Library Svcs
ATTN: R. Halprin

Meteor Communications Corp
ATTN: R. Leader

Mission Research Corp
ATTN: R. Bigoni
ATTN: F. Guigliano
ATTN: C. Lauer
ATTN: D. Archer
ATTN: Tech Library
ATTN: S. Gutsche
ATTN: R. Hendrick
ATTN: C. Longmire
ATTN: G. McCarton
ATTN: D. Knepp
ATTN: M. Scheibe
ATTN: R. Bogusch
ATTN: R. Kilb
ATTN: F. Fajen
4 cy ATTN: R. Christian
4 cy ATTN: T. Barrett
5 cy ATTN: Doc Control

SRI International
ATTN: F. Perkins

DEPARTMENT OF DEFENSE CONTRACTORS (Continued)

Mitre Corp
ATTN: MS J104/M, R. Dresp

Mitre Corp
ATTN: J. Wheeler
ATTN: W. Hall
ATTN: W. Foster

Nichols Research Corp, Inc
ATTN: N. Byrn
ATTN: W. Mendes
ATTN: J. Smith

Pacific-Sierra Resrarch Corp
ATTN: H. Brode, Chairman SAGE

Photometrics, Inc
ATTN: I. Kofsky

Physical Dynamics, Inc
ATTN: E. Fremouw

Physical Research, Inc
ATTN: R. Deliberis
ATTN: T. Stephens

University of the Commonwealth, Pittsburgh
ATTN: F. Kaufman

R&D Associates
ATTN: M. Gantsweg
ATTN: H. Ory
ATTN: R. Turco
ATTN: W. Karzas
ATTN: F. Gilmore
ATTN: P. Haas

R&D Associates
ATTN: B. Yoon

Rand Corp
ATTN: C. Crain
ATTN: E. Bedrozian
ATTN: P. Davis

Rand Corp
ATTN: B. Bennett

Raytheon Co
ATTN: G. Thome

Riverside Research Intitute
ATTN: V. Trapani

Science Applications, Inc
ATTN: C. Smith
ATTN: R. Lee
ATTN: D. Hamlin
ATTN: L. Linson

Science Applications, Inc
ATTN: J. Cockayne

Science Applications, Inc
ATTN: M. Cross

Stewart Radiance Lab
ATTN: J. Ulwick

DEPARTMENT OF DEFENSE CONTRACTORS (Continued)

SRI International

ATTN: R. Hake Jr
ATTN: R. Leadabrand
ATTN: R. Leonard
ATTN: W. Chesnut
ATTN: V. Gonzales
ATTN: J. Casper
ATTN: W. Jaye
ATTN: J. Depp
ATTN: G. Smith
ATTN: A. Burns
ATTN: R. Tsunoda
ATTN: J. Vickrey
ATTN: M. Baron
ATTN: D. McDaniels
ATTN: C. Rino

Teledyne Brown Engineering

ATTN: J. Cato
ATTN: G. Harney
ATTN: F. Leopard
ATTN: N. Passino
ATTN: MS-12, Tech Library

DEPARTMENT OF DEFENSE CONTRACTORS (Continued)

Technology International Corp

ATTN: W. Boquist

Toyon Research Corporation

ATTN: J. Ise
ATTN: J. Garbarino

TRW Electronics & Defense Sector

ATTN: R. Plebuch
ATTN: G. Kirchner

Utah State University

Attention Sec Con Ofc for
ATTN: A. Steed
ATTN: D. Burt

Visidyne, Inc

ATTN: O. Shepard
ATTN: J. Carpenter
ATTN: H. Smith
ATTN: C. Humphrey
ATTN: W. Reidy

